Supporting Information for

The discrete breast cancer stem cell mammosphere activity of Group 10-bis(azadiphosphine) metal complexes

Zhiyin Xiao,[a,b†] Alice Johnson,[a†] Kuldip Singh,[a] and Kogularamanan Suntharalingam[a]*

[a] School of Chemistry, University of Leicester, Leicester, UK
[b] College of Biological, Chemical Sciences and Engineering, Jiaxing University, Jiaxing, China

† These authors contributed equally to this work
* To whom correspondence should be addressed:
Email: k.suntharalingam@leicester.ac.uk

Table of Content

Experimental Details

Materials and Methods. All synthetic procedures were performed under normal atmospheric conditions or under nitrogen. Fourier transform infrared (FTIR) spectra were recorded with an IRAffinity-1S Shimadzu spectrophotometer. Electron spray ionisation mass spectra were recorded on a Micromass Quattro spectrometer. UV-vis absorption spectra were recorded on a Cary 3500 UV-Vis spectrophotometer. ^{1}H, ^{13}C, ^{19}F, and ^{31}P NMR spectra were recorded on a BrukerAvance 400 MHz Ultrashield NMR spectrometer. ^{1}H NMR spectra were referenced internally to residual solvent peaks, and chemical shifts are expressed relative to tetramethylsilane, $SiMe_4$ (δ = 0 ppm). Elemental analysis of the compounds prepared was performed commercially by London Metropolitan University. Chlorodiphenylphosphine, *n*-hexylamine, $[Ni(H_2O)_6](BF_4)_2$, $[Pd(NCMe)_4](BF_4)_2$, [Pt(1,5-cyclooctadiene)Cl_2], and $NaBF_4$ were purchased from Sigma Aldrich or Alfa Aesar and used as received.

Synthesis of L^{1}. Chlorodiphenylphosphine (3.6 mL, 20 mmol) was slowly added to a solution of *n*-hexylamine (1.35 mL, 10 mmol) and triethylamine (3.6 mL, 26 mmol) in CH_2C1_2 (20 mL) under N_2 atmosphere at 0 °C. The mixture was then stirred at ambient temperature overnight. The resulting precipitates ($Et_3N{\cdot}HCl$ salts) were removed by filtration through silica, using DCM as the eluent. Upon removal of DCM under vacuum, **L^{1}** was isolated as a white solid (3.7987 g, 81%); ^{1}H NMR (400 MHz, $CDCl_3$): δ 7.46 – 7.36 (m, 8H, Ar-*H*), 7.36 – 7.27 (m, 12H, Ar-*H*), 3.32 – 3.15 (m, 2H, C*H*$_2$), 1.18 – 1.01 (m, 4H, 2×C*H*$_2$), 1.01 – 0.83 (m, 4H, 2×C*H*$_2$), 0.76 (t, *J* = 7.2 Hz, 3H, C*H*$_3$); ^{13}C NMR (101 MHz, $CDCl_3$): δ 139.81 (t, *J* = 6.1 Hz), 132.86 (t, *J* = 11.1 Hz), 128.81 (s), 128.15 (t, *J* = 3.0 Hz), 53.24 (t, *J* = 11.1 Hz), 31.43 (s), 31.41 (s), 26.53 (s), 22.58 (s), 14.05 (s); ^{31}P NMR (162 MHz, $CDCl_3$): δ 62.13 (s); UV–vis (1-octanol, λ_{max} / nm): 254; IR (solid, ATR, cm^{-1}): 3071, 2910, 2853, 1478, 1366, 1090, 1064, 1025, 899, 852, 783, 738, 692, 644, 504, 454, 440; HR-ESI MS Calcd. for $C_{30}H_{34}NP_2$ $[M+H]^+$: 470.5073 a.m.u. Found $[M+H]^+$: 470.2166 a.m.u.; Anal. Calcd. for $C_{30}H_{33}NP_2$ (%): C, 76.74; H, 7.08; N, 2.98. Found: C, 76.59; H, 7.16; N, 3.06.

Synthesis of the nickel(II)-bis(azadiphosphine) complex, 1. A DCM solution (5 mL) containing **L^{1}** (126 mg, 0.27 mmol) was added to an acetonitrile solution (5 mL) containing $[Ni(H_2O)_6](BF_4)_2$ (44 mg, 0.13 mmol). The reaction mixture was stirred for 4 h at ambient temperature. Upon removal of the solvent under vacuum, the resultant residue was washed with diethyl ether (3 mL × 2). Solvent-layer diffusion of hexane into a DCM solution containing the washed solid enabled isolation of **1** as yellow crystals (130 mg, 86%). ^{1}H NMR (400 MHz, $CDCl_3$): δ 7.63 (t, *J* = 7.2 Hz, 4H, Ar-*H*), 7.57 (t, *J* = 7.3 Hz, 8H, Ar-*H*), 7.50 (d, *J* = 3.0 Hz, 8H, Ar-*H*), 2.79 (dp, *J* = 19.0, 6.4 Hz, 2H, C*H*$_2$), 1.11 – 0.99 (m, 2H, C*H*$_2$), 0.99 – 0.88 (m, 2H, C*H*$_2$), 0.88 – 0.70 (m, 4H, 2×C*H*$_2$), 0.65 (t, *J* = 7.2 Hz, 3H, C*H*$_3$); ^{13}C NMR (101 MHz, $CDCl_3$): δ 134.59 (s), 133.02 (t, *J* = 3.0 Hz), 130.88 (s, *J* = 3.0 Hz), 124.55 (t, *J* = 14.6 Hz), 49.18 (s), 30.80 (s), 29.44 (s), 26.50 (s), 22.27 (s), 13.81 (s); ^{31}P NMR (162 MHz, $CDCl_3$): δ 58.88 (s); ^{19}F NMR (376 MHz, $CDCl_3$): δ -152.06 (s), -152.11 (s); UV–vis (1-octanol, λ_{max} / nm): 267, 304, 336; IR (solid, ATR, cm^{-1}): 3054, 2922, 2854, 1584, 1478, 1435, 1093, 1050, 997, 899, 850, 822, 747, 692, 631, 545, 510, 464, 441; HR-ESI MS Calcd. for $C_{60}H_{66}N_2P_4Ni$ $[M-2BF_4]^{2+}$: 498.8460 a.m.u. Found $[M-2BF_4]^{2+}$: 498.1802 a.m.u.; Anal. Calcd. for $C_{60}H_{66}N_2P_4B_2F_8Ni$ (%): C, 61.52; H, 5.68; N, 2.39. Found: C, 61.08; H, 5.35; N, 2.40.

Synthesis of the palladium(II)-bis(azadiphosphine) complex, 2. A DCM solution (5 mL) containing **L^{1}** (192.8 mg, 0.41 mmol) was added to a DCM solution (8 mL) containing $[Pd(NCMe)_4](BF_4)_2$ (89 mg, 0.20 mmol). The reaction mixture was stirred for 1 h at ambient

temperature. Upon removal of the solvent under vacuum, the resultant residue was washed with diethyl ether (3 mL × 2). Solvent-layer diffusion of hexane into a DCM solution containing the washed solid enabled isolation of **2** as yellow crystals (217 mg, 89%). ^{1}H NMR (400 MHz, $CDCl_3$): δ 7.67 (t, *J* = 7.4 Hz, 4H, Ar-*H*), 7.57 (t, *J* = 7.5 Hz, 8H, Ar-*H*), 7.48 (dd, *J* = 6.5, 3.3 Hz, 8H, Ar-*H*), 2.92 (dp, *J* = 13.7, 6.9 Hz, 2H, C*H*$_2$), 1.04 (dt, *J* = 14.4, 7.4 Hz, 2H, C*H*$_2$), 0.99 – 0.88 (m, 2H, C*H*$_2$), 0.88 – 0.71 (m, 4H, 2×C*H*$_2$), 0.66 (t, *J* = 7.2 Hz, 3H, C*H*$_2$); ^{13}C NMR (101 MHz, $CDCl_3$): δ 134.61 (s), 133.34 – 132.70 (m), 131.27 – 130.54 (m), 125.16 – 124.21 (m), 50.31 (s), 30.79 (s), 29.50 (s), 26.45 (s), 22.25 (s), 13.81 (s); ^{31}P NMR (162 MHz, $CDCl_3$): δ 46.65 (s); ^{19}F NMR (376 MHz, $CDCl_3$) δ -152.20 (s), -152.25 (s); UV–vis (1-octanol, λ_{max} / nm): 251, 325; IR (solid, ATR, cm^{-1}): 3054, 2956, 2861, 1585, 1479, 1436, 1097, 1047, 996, 898, 847, 821, 747, 691, 627, 611, 544, 508, 499, 465; HR-ESI MS Calcd. for $C_{60}H_{66}N_2P_4Pd$ $[M\text{-}2BF_4]^{2+}$: 522.7094 a.m.u. Found $[M\text{-}2BF_4]^{2+}$: 522.1621 a.m.u.; Anal. Calcd. for $C_{60}H_{66}N_2P_4B_2F_8Pd$ (%): C, 59.11; H, 5.46; N, 2.30. Found: C, 59.20; H, 5.49; N, 2.61.

Synthesis of the platinum(II)-bis(azadiphosphine) complex, 3. A DCM solution (1.5 mL) containing [Pt(1,5-cyclooctadiene)Cl_2] (37.5 mg, 0.1 mmol) was added to a DCM:MeOH (1:1) solution (8 mL) containing **L^1** (95.2 mg, 0.2 mmol) and $NaBF_4$ (23 mg, 0.2 mmol). The reaction mixture was stirred for 30 min at ambient temperature. Upon removal of the solvent under vacuum, the resultant residue was washed with diethyl ether (4 mL × 3). The resultant white solid was dissolved into DCM (2 mL) and filtered through Celite 545 to remove NaCl salts (by-products). The solvent was removed under vacuum. Solvent-layer diffusion of hexane into a DCM solution containing the solid from the previous step enabled isolation of **3** as colourless crystals (112 mg, 86%); ^{1}H NMR (400 MHz, $CDCl_3$): δ 7.68 (t, *J* = 7.4 Hz, 4H, Ar-*H*), 7.58 (t, *J* = 7.5 Hz, 8H, Ar-*H*), 7.53 – 7.40 (m, 8H, Ar-*H*), 2.81 (dp, *J* = 13.7, 6.8 Hz, 2H, C*H*$_2$), 1.11 – 1.00 (m, 2H, C*H*$_2$), 1.00 – 0.89 (m, 2H, C*H*$_2$), 0.86 – 0.71 (m, 4H, 2×C*H*$_2$), 0.66 (t, *J* = 7.2 Hz, 3H, C*H*$_3$); ^{13}C NMR (101 MHz, $CDCl_3$): δ 134.87 (s), 133.07 (t, *J* = 3.0 Hz), 130.86 (t, *J* = 3.0 Hz), 124.29 (t, *J* = 17.2 Hz), 51.37 (s), 30.80 (s), 29.33 (s), 26.46 (s), 22.26 (s), 13.82 (s); ^{31}P NMR (162 MHz, $CDCl_3$): δ 39.97 (t, *J* = 1077.3 Hz); ^{19}F NMR (376 MHz, $CDCl_3$): δ -152.42 (s), -152.47 (s); UV–vis (1-octanol, λ_{max} / nm): 264; IR (solid, ATR, cm^{-1}): 3052, 2924, 2857, 1585, 1479, 1436, 1310, 1282, 1097, 1045, 996, 903, 863, 840, 797, 746, 723, 689, 631, 614, 545, 511, 498, 440; HR-ESI MS Calcd. for $C_{60}H_{66}N_2P_4Pt$ $[M\text{-}2BF_4]^{2+}$: 567.03931 a.m.u. Found $[M\text{-}2BF_4]^{2+}$: 566.6943 a.m.u.; Anal. Calcd. For $C_{60}H_{66}N_2P_4B_2F_8Pt$ (%): C, 55.11; H, 5.09; N, 2.14. Found: C, 54.90; H, 5.17; N, 2.17.

Synthesis of L^{1}O. A THF solution (3 mL) containing H_2O_2 (13.1 mg of 30wt%, 0.11 mmol) was added to a THF solution (5 mL) containing **L^1** (48.7 mg, 0.10 mmol) under an ice-bath. The reaction mixture was stirred for 1 h. Upon removal of the solvent under vacuum, the resultant residue was separated using thin-layer chromatography with ethyl acetate as an eluent. A desired product, **L^{1}O** was isolated as a colourless liquid (33 mg, 62%); ^{1}H NMR (400 MHz, $CDCl_3$) δ 8.01 – 7.81 (m, 4H, Ar-*H*), 7.55 – 7.31 (m, 16H, Ar-*H*), 3.30 (ddd, *J* = 16.5, 10.9, 2.7 Hz, 2H, CH_2), 0.98 – 0.63 (m, 11H, 5×C*H*$_2$ + C*H*$_3$); ^{13}C NMR (101 MHz, $CDCl_3$): δ 136.84 (dd, *J* = 16.8, 5.1 Hz), 134.05 (d, *J* = 4.0 Hz), 132.96 (s), 132.76 (s), 132.55 (dd, *J* = 9.5, 3.1 Hz), 131.84 (d, *J* = 2.8 Hz), 129.37 (s), 128.44 (dd, *J* = 14.2, 9.4 Hz), 47.65 (s), 31.04 (s), 30.91 (s), 26.61 (s), 22.40 (s), 13.96 (s); ^{31}P NMR (162 MHz, $CDCl_3$): δ 49.10 (d, *J* = 87.3 Hz), 32.95 (d, *J* = 87.3 Hz); ^{1}H NMR (400 MHz, DMSO-d^6): δ 7.95 – 7.81 (m, 4H, Ar-*H*), 7.64 – 7.34 (m, 8H, Ar-*H*), 3.19 – 3.09 (m, 2H, C*H*$_2$), 0.82 (dt, *J* = 13.9, 7.0 Hz, 2H, C*H*$_2$), 0.70 – 0.56 (m, 7H, 2×C*H*$_2$ + C*H*$_3$), 0.52 (dd, *J* = 13.5, 6.7 Hz, 2H, C*H*$_2$); ^{31}P NMR (162 MHz, DMSO-d^6): δ 47.72 (d, *J* = 83.3 Hz), 29.86 (d, *J* = 83.3 Hz); ESI MS Calcd. for $C_{30}H_{34}NOP_2$ $[M+H]^+$: 486.21 a.m.u. Found $[M+H]^+$: 486 a.m.u.

Synthesis of L^1OO. A THF solution (1 mL) containing H_2O_2 (58.4 mg of 30wt%, 0.47 mmol) was added to a THF solution (5 mL) containing $\mathbf{L^1}$ (105.3 mg, 0.22 mmol). The reaction mixture was stirred for 30 min at ambient temperature. Upon removal of the solvent under vacuum, the resultant residue was washed with diethyl hexane (3 mL × 2) to yield $\mathbf{L^1OO}$ as colourless viscous liquid (93.2 mg, 83%); ^{1}H NMR (400 MHz, $CDCl_3$): δ 7.86 – 7.73 (m, 8H, Ar-*H*), 7.43 – 7.34 (m, 4H, Ar-*H*), 7.29 (td, *J* = 7.5, 3.1 Hz, 8H, Ar-*H*), 3.30 – 3.15 (m, 2H, C*H*$_2$), 1.37 (dt, *J* = 15.4, 7.6 Hz, 2H, C*H*$_2$), 1.01 – 0.89 (m, 2H, C*H*$_2$), 0.78 (ddd, *J* = 13.9, 8.8, 6.7 Hz, 2H, C*H*$_2$), 0.73 – 0.62 (m, *J* = 14.6, 7.1 Hz, 5H, C*H*$_2$ + C*H*$_3$); ^{13}C NMR (101 MHz, $CDCl_3$): δ 132.94 – 132.45 (m), 131.87 (s), 131.75 (d, *J* = 117.2 Hz), 128.35 – 127.80 (m), 47.61 (s), 31.18 (s), 30.78 (s), 26.23 (s), 22.33 (s), 13.89 (s). ^{31}P NMR (162 MHz, $CDCl_3$): δ 29.42; ^{1}H NMR (400 MHz, DMSO-d^6): δ 10.21 (s, 1H, O*H*), 7.80 – 7.63 (m, 8H, Ar-*H*), 7.57 – 7.48 (m, 4H, Ar-*H*), 7.43 (td, *J* = 7.5, 3.1 Hz, 8H, Ar-*H*), 3.25 – 3.10 (m, 2H, C*H*$_2$), 1.16 – 1.03 (m, 2H, C*H*$_2$), 0.96 – 0.82 (m, 2H, C*H*$_2$), 0.76 – 0.57 (m, 7H, 2×C*H*$_2$ + C*H*$_3$); ^{31}P NMR (162 MHz, DMSO-d^6): δ 28.71 (s); IR (solid, ATR, cm^{-1}):3276, 3057, 2956, 2928, 2854, 1590, 1483, 1437, 1210, 1119, 1110, 1366, 1054, 1025, 996, 925, 865, 729, 688, 565, 513, 448; ESI MS Calcd. for $C_{30}H_{34}NO_2P_2$ $[M+H]^+$: 502.21 a.m.u. Found $[M+H]^+$: 502 a.m.u.

X-ray Single Crystal Diffraction Analysis. Single crystals of complexes **1-3** were obtained by layer-diffusion of hexane into a DCM solution of the metal complex. Crystals suitable for X-ray diffraction analysis were selected and mounted on a Bruker Apex 2000 CCD area detector diffractometer using standard procedures. Data was collected using graphite-monochromated Mo-Kα radiation (λ = 0.71073) at 150(2) K. Crystal structures were solved and refined using the Bruker SHELXTL software.[1] All hydrogen atoms were located by geometrical calculations, and all non-hydrogen atoms were refined anisotropically. The structures have been deposited with the Cambridge Crystallographic Data Centre (CCDC 2035446-2035448). This information can be obtained free of charge from www.ccdc.cam.ac.uk/data_request/cif.

Measurement of water-octanol partition coefficient (LogP). The LogP values for **1-3** were determined using the shake-flask method and UV-vis spectroscopy. The 1-octanol used in this experiment was pre-saturated with water. An aqueous solution of **1-3** (500 μL, 100 μM) was incubated with 1-octanol (500 μL) in a 1.5 mL tube. The tube was shaken at room temperature for 2 h. The two phases were separated by centrifugation and the **1-3** content in each phase was determined by UV-vis spectroscopy.

Cell Lines and Cell Culture Conditions. The human mammary epithelial cell line, HMLER-shEcad was kindly donated by Prof. R. A. Weinberg (Whitehead Institute, MIT). HMLER-shEcad cells were maintained in Mammary Epithelial Cell Growth Medium (MEGM) with supplements and growth factors (BPE, hydrocortisone, hEGF, insulin, and gentamicin/amphotericin-B). The cells were grown at 310 K in a humidified atmosphere containing 5% CO_2.

Monolayer Cytotoxicity Studies. The colorimetric MTT assay was used to determine the IC_{20} values of **1-3** against CSC-enriched HMLER-shEcad cells. HMLER-shEcad cells (5×10^3) were seeded in each well of a 96-well plate. After incubating the cells overnight, various concentrations of the compounds (0.2-100 μM), were added and incubated for 72 h (total volume 200 μL). Stock solutions of the compounds were prepared as 10 mM solutions in DMSO and diluted using media. The final concentration of DMSO in each well was 0.5%

and this amount was present in the untreated control as well. After 72 h, 20 µL of a 4 mg/mL solution of MTT in PBS was added to each well, and the plate was incubated for an additional 4 h. The MEGM/MTT mixture was aspirated and 200 µL of DMSO was added to dissolve the resulting purple formazan crystals. The absorbance of the solutions in each well was read at 550 nm. Absorbance values were normalized to (DMSO-containing) control wells and plotted as concentration of test compound versus % cell viability (see Figure below). IC_{20} values were interpolated from the resulting dose dependent curves. The reported IC_{20} values are the average of three independent experiments (n = 18) (see Table below).

Representative dose-response curves for the treatment of HMLER-shEcad cells with **1**-**3** after 72 h incubation:

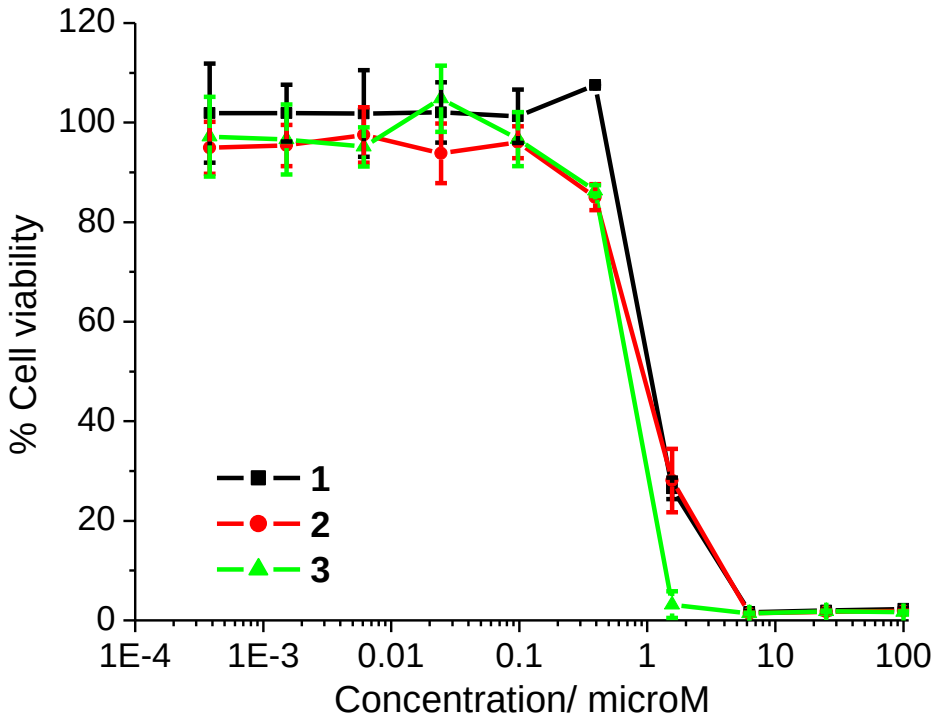

IC_{20} values of **1**-**3** against HMLER-shEcad cells (mean of three independent experiments ± SD):

Metal complex	HMLER-shEcad IC_{20} [µM]
1	0.59 ± 0.01
2	0.45 ± 0.02
3	0.43 ± 0.01

Mammosphere Formation and Viability Assay. HMLER-shEcad cells (5×10^3) were plated in ultralow-attachment 96-well plates (Corning) and incubated in MEGM supplemented with B27 (Invitrogen), 20 ng/mL EGF, and 4 µg/mL heparin (Sigma) for 5 days. Studies were also conducted in the presence of **1-3**, $\mathbf{L^1}$, and salinomycin (0-133 µM). Mammospheres treated with **1-3** or salinomycin (at their respective IC_{20} values, 5 days), or $\mathbf{L^1}$ (at 133 µM, 5 days) were counted and imaged using an inverted microscope. The viability of

the mammospheres was determined by addition of a resazurin-based reagent, TOX8 (Sigma). The fluorescence of the solutions was read at 590 nm (λ_{ex} = 560 nm). Viable mammospheres reduce the amount of the oxidized TOX8 form (blue) and concurrently increases the amount of the fluorescent TOX8 intermediate (red), indicating the degree of mammosphere cytotoxicity caused by the test compound. Fluorescence values were normalized to DMSO-containing controls and plotted as concentration of test compound versus % mammospheres viability. IC_{50} values were extrapolated from the resulting dose dependent curves. The reported IC_{50} values are the average of three independent experiments.

Mammosphere Uptake. To measure the cellular uptake of **2** and **3**, *ca.* 5 x 10^4 HMLER-shEcad mammospheres were treated with **2** or **3** at a non-lethal dose (1 μM for 6 h, at 37 °C). After incubation, the mammospheres were counted and harvested. The mammosphere pellets were dissolved in 65% HNO_3 (250 μL) overnight. Pellets of **2** and **3** treated HMLER-shEcad mammospheres were also used to determine the palladium and platinum content in the nuclear, cytoplasmic, and membrane fractions of HMLER-shEcad cells (making up the mammospheres). The Thermo Scientific NE-PER Nuclear and Cytoplasmic Extraction Kit was used to extract and separate the nuclear, cytoplasmic, and membrane fractions. The fractions were dissolved in 65% HNO_3 overnight (250 μL final volume). All samples were analysed using inductively coupled plasma mass spectrometry (ICP-MS, ThermoScientific ICAP-Qc quadrupole ICP mass spectrometer). Palladium or platinum levels are expressed as Pd or Pd (ng) per 10^3 mammospheres. Results are presented as the mean of four determinations for each data point.

Immunoblotting Analysis. HMLER-shEcad mammospheres (5×10^4) were incubated with **2** or **3** (IC_{50} value for 72 h) at 37 ^oC. Mammospheres were harvested and isolated as pellets. SDS-PAGE loading buffer (64 mM Tris-HCl (pH 6.8)/ 9.6% glycerol/ 2%SDS/ 5% β-mercaptoethanol/ 0.01% Bromophenol Blue) was added to the mammospheres pellets, and this was incubated at 95 ^oC for 10 min. Mammosphere lysates were resolved by 4-20 % sodium dodecylsulphate polyacylamide gel electrophoresis (SDS-PAGE; 200 V for 25 min) followed by electro transfer to polyvinylidene difluoride membrane, PVDF (350 mA for 1 h). Membranes were blocked in 5% (w/v) non-fat milk in PBST (PBS/0.1% Tween 20) and incubated with the appropriate primary antibodies (Cell Signalling Technology). After incubation with horseradish peroxidase-conjugated secondary antibodies (Cell Signalling Technology), immune complexes were detected with the ECL detection reagent (BioRad) and analysed using a chemiluminescence imager (Bio-Rad ChemiDoc Imaging System).

Ethidium Bromide Displacement Studies. To a mixture of ethidium bromide (1 μM) and ct-DNA (20 μM) in 5 mM Tris–HCl (pH 7.4) buffer (with a total volume of 2 mL) an increasing amount of **2** or **3** (0-100 μM) was added in aliquots, from a 10 mM stock solution of **2** or **3**. The solution was incubated at room temperature for 30 seconds after each aliquot addition of **2** or **3** and then the emission spectrum was recorded between 550 and 800 nm with an excitation wavelength of 526 nm. The fluorescence intensity at λ_{max} was used to determine the quenching constant of **2** or **3**. The quenching constant (K_q) was determined using the Stern-Volmer equation: $F^o/F = K_q[Q] + 1$, where F^o is the emission intensity of ct-DNA and ethidium bromide in the absence of **2** or **3**, F is the emission intensity in the presence of **2** or **3**, K_q is the quenching constant, and [Q] is the concentration of **2** or **3**. The quenching constant was extrapolated from F^o/F versus [Q] plots. The experiment was conducted three times, independently. The reported quenching constant is the average of the three values obtained from the three independent experiments.

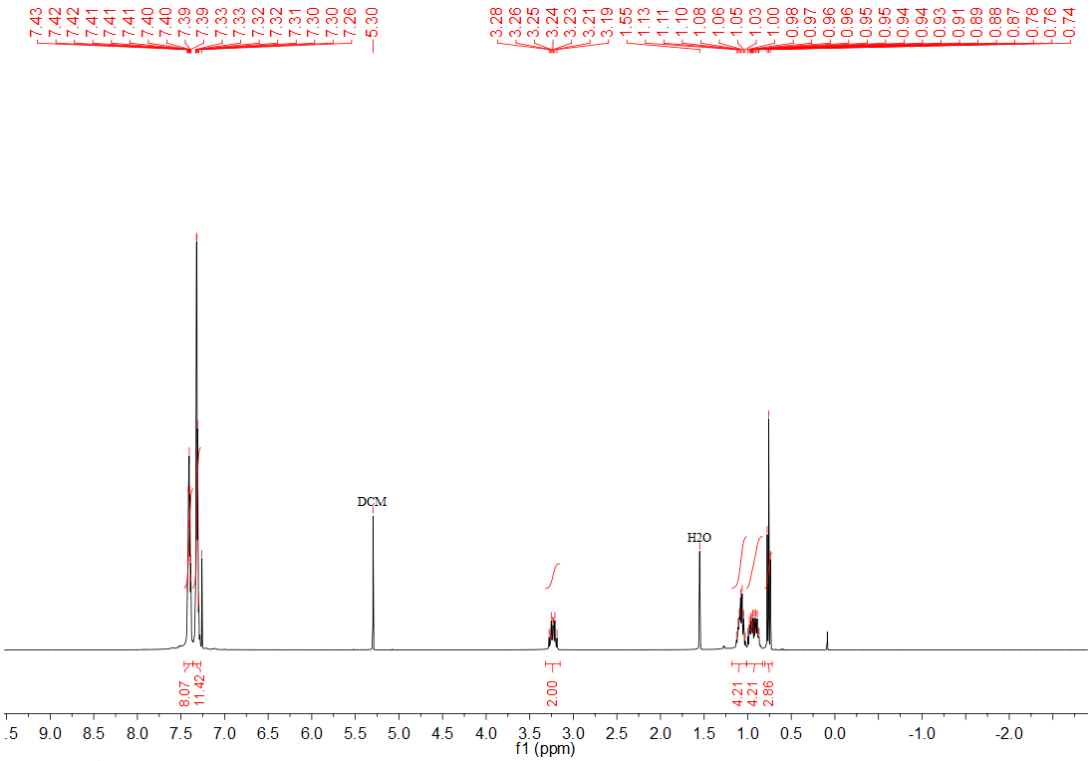

Figure S1. ^{1}H NMR spectrum of **L^{1}** in $CDCl_3$.

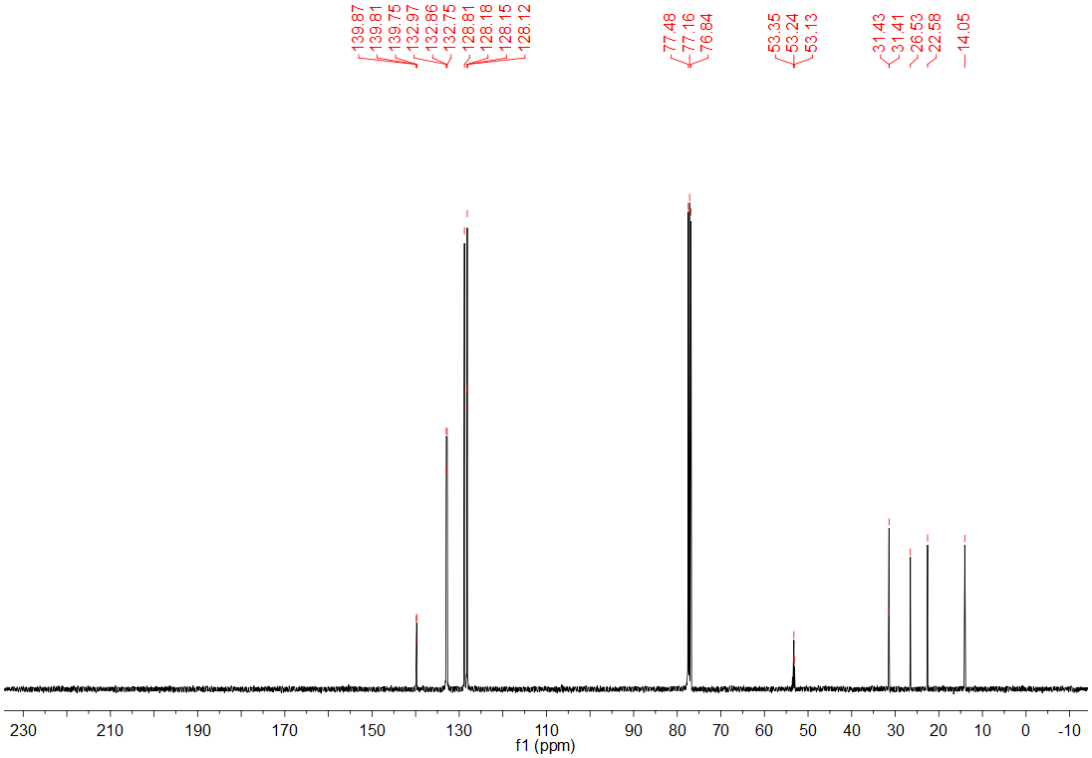

Figure S2. $^{13}C\{^{1}H\}$ NMR spectrum of **L^{1}** in $CDCl_3$.

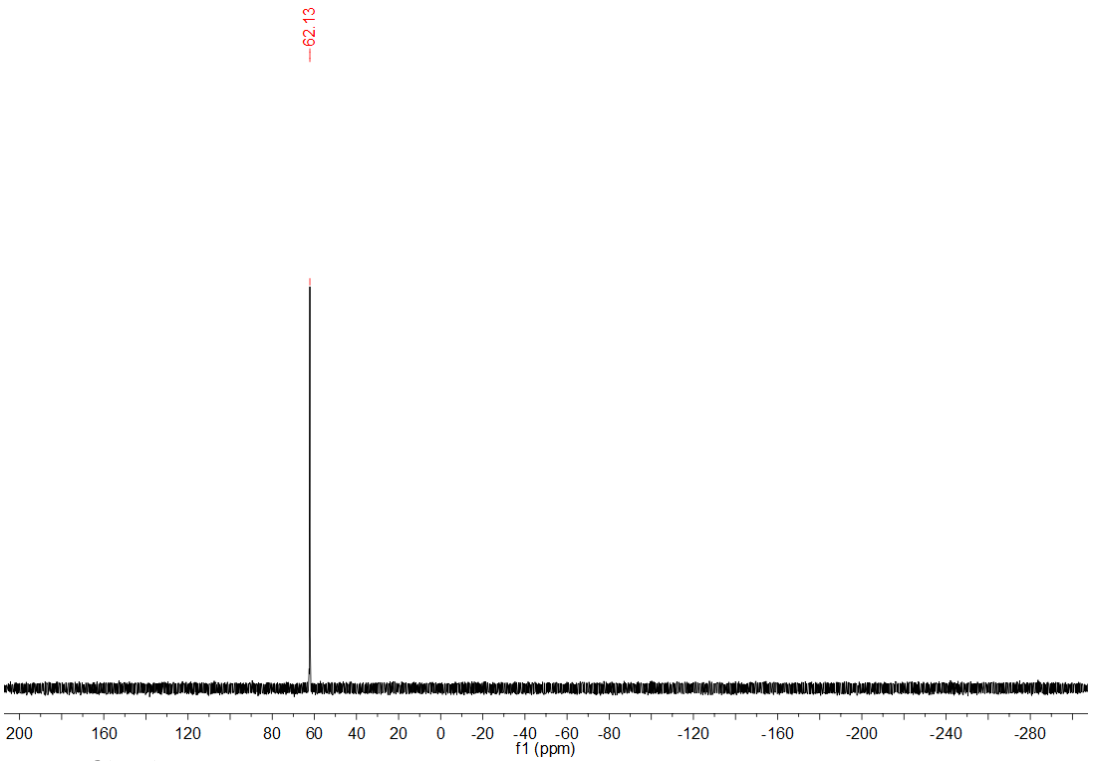

Figure S3. $^{31}P\{^{1}H\}$ NMR spectrum of **L¹** in $CDCl_3$.

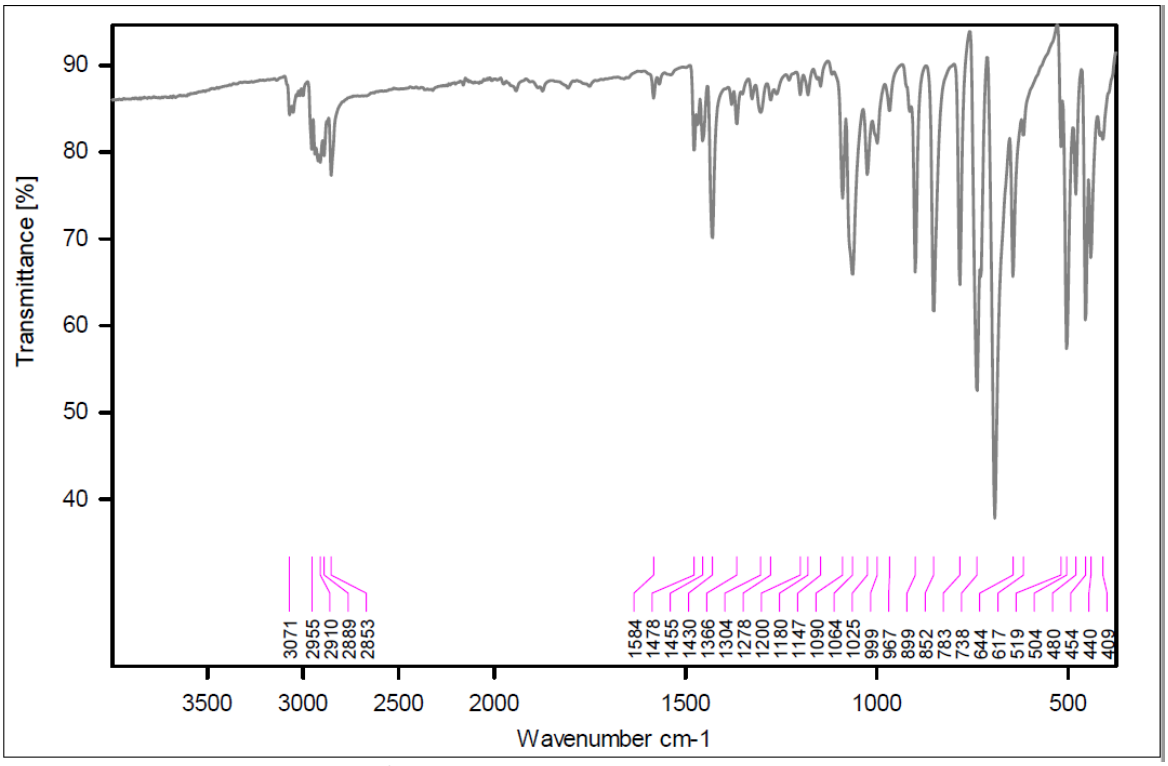

Figure S4. ATR spectrum of **L¹** in the solid form.

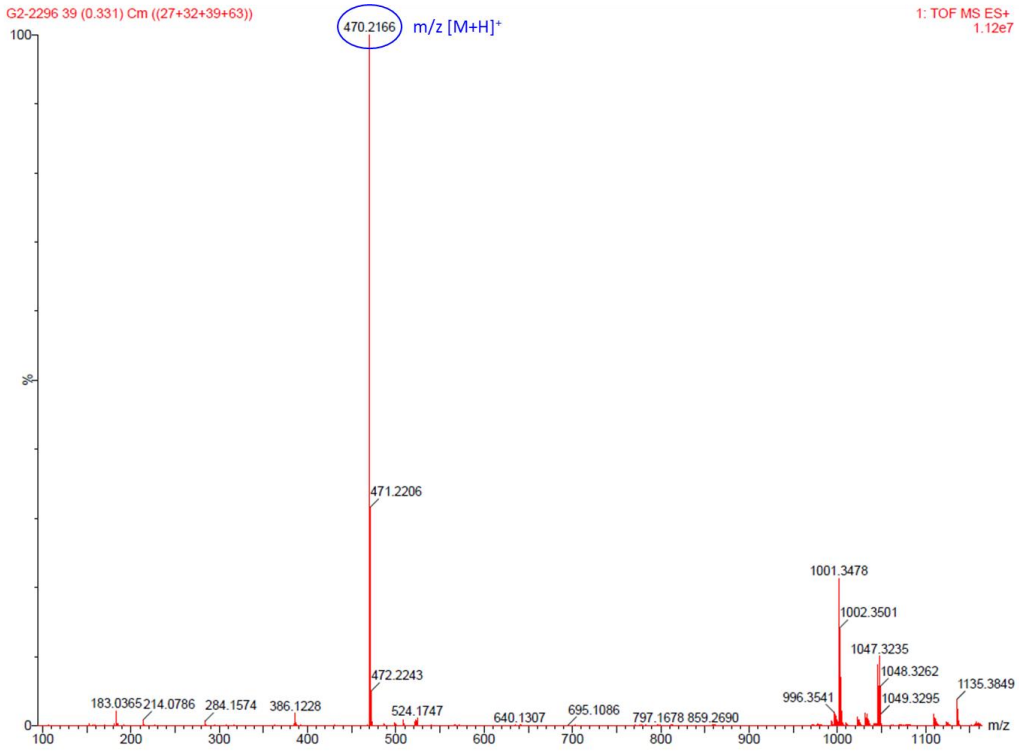

Figure S5. HR-ESI mass spectrum (positive mode) of **L**[1].

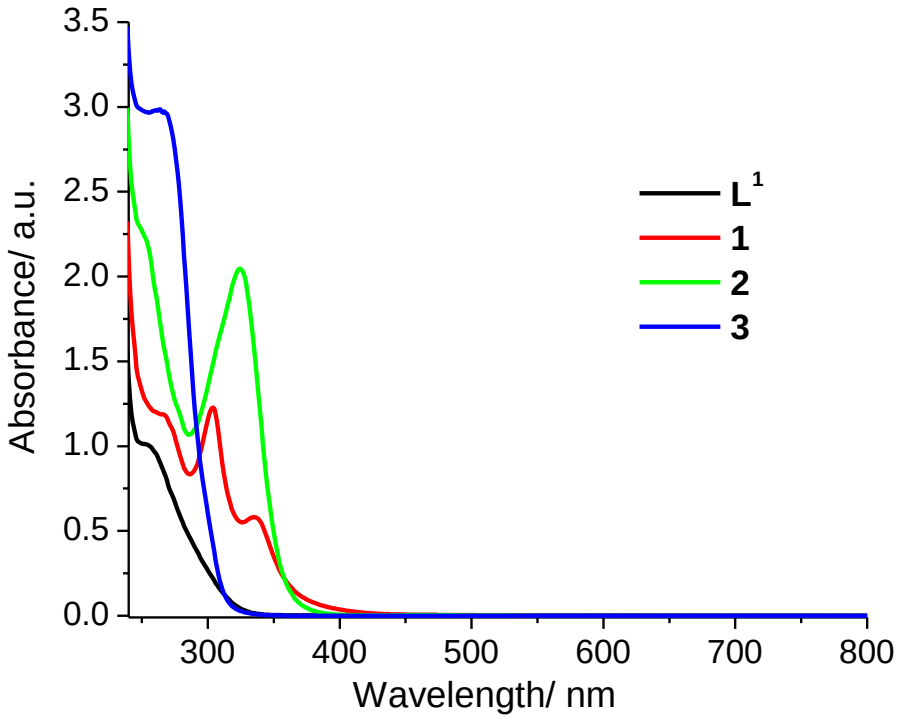

Figure S6. UV-vis spectrum of **1-3** and **L**[1] (50 μM) in 1-octanal.

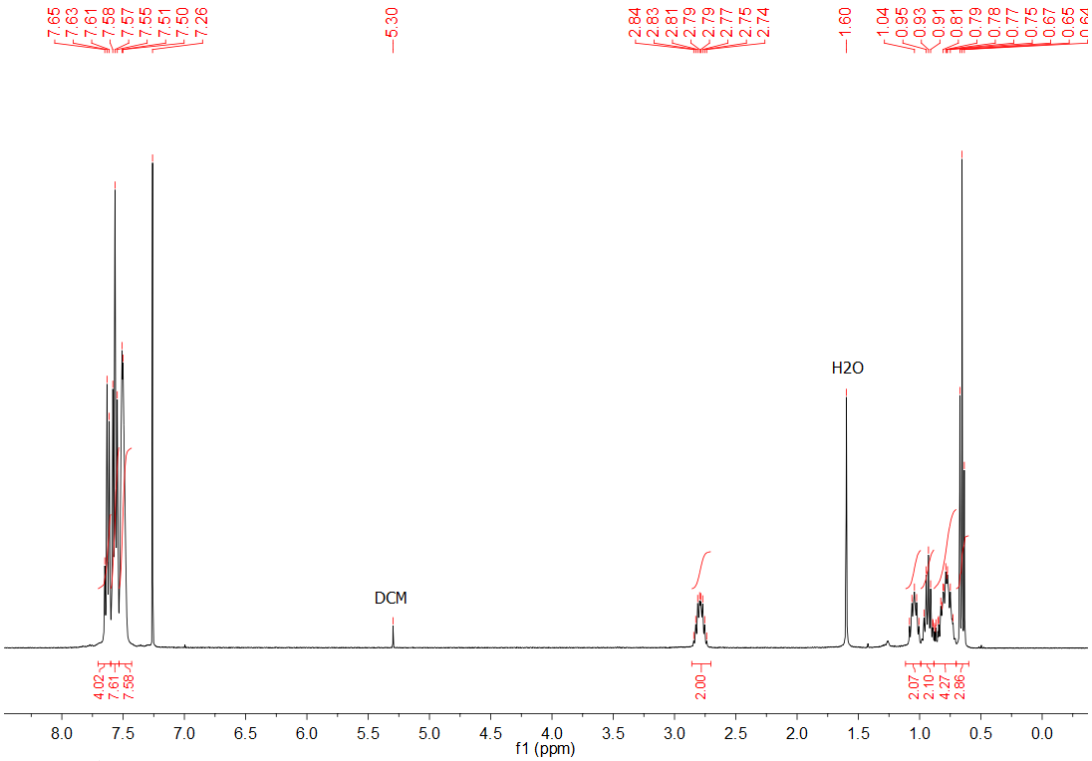

Figure S7. ^{1}H NMR spectrum of **1** in $CDCl_3$.

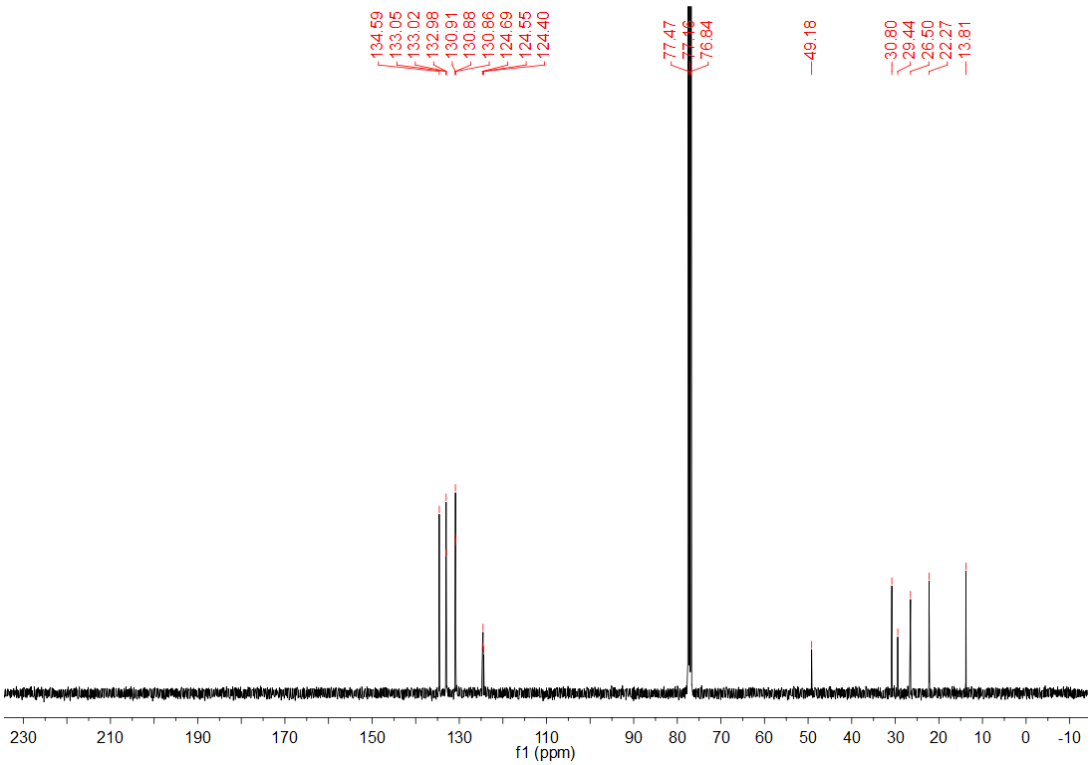

Figure S8. $^{13}C\{^{1}H\}$ NMR spectrum of **1** in $CDCl_3$.

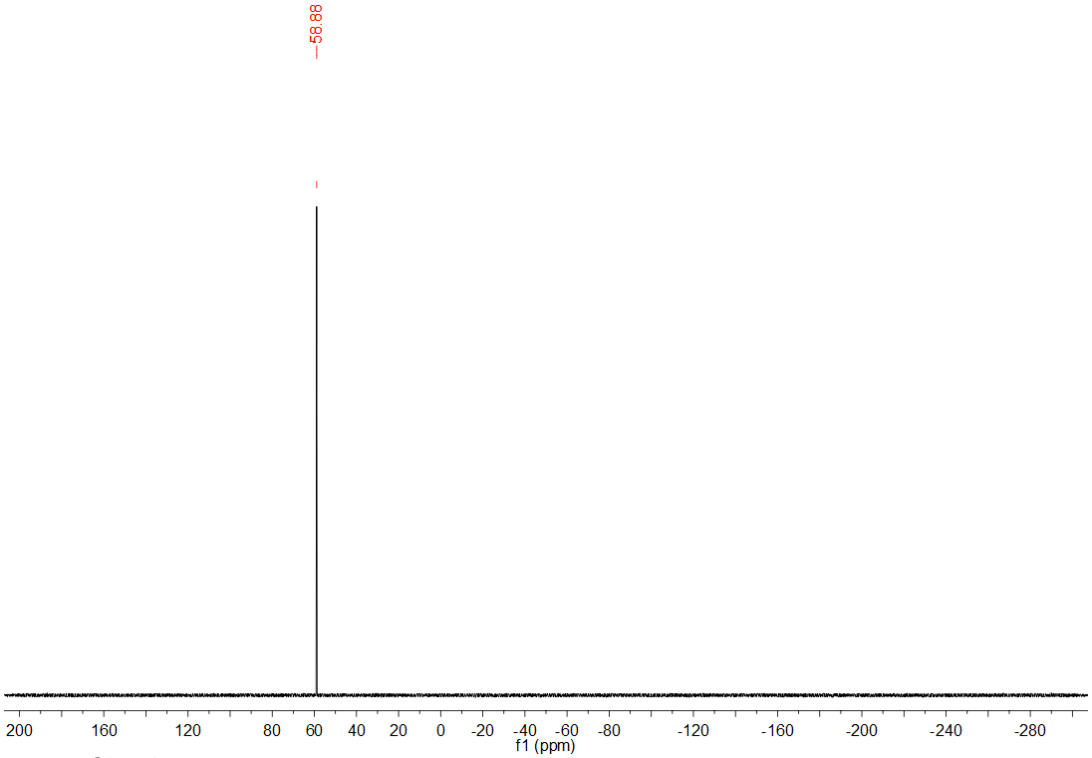

Figure S9. $^{31}P\{^{1}H\}$ NMR spectrum of **1** in $CDCl_3$.

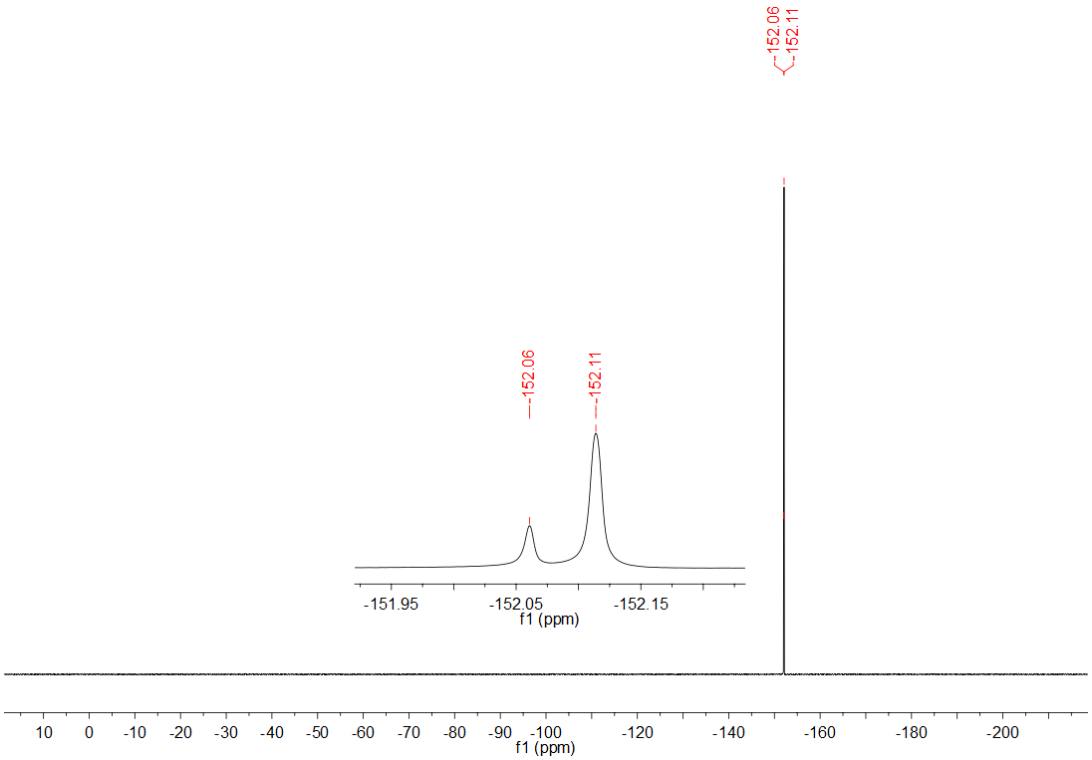

Figure S10. $^{19}F\{^{1}H\}$ NMR spectrum of **1** in $CDCl_3$.

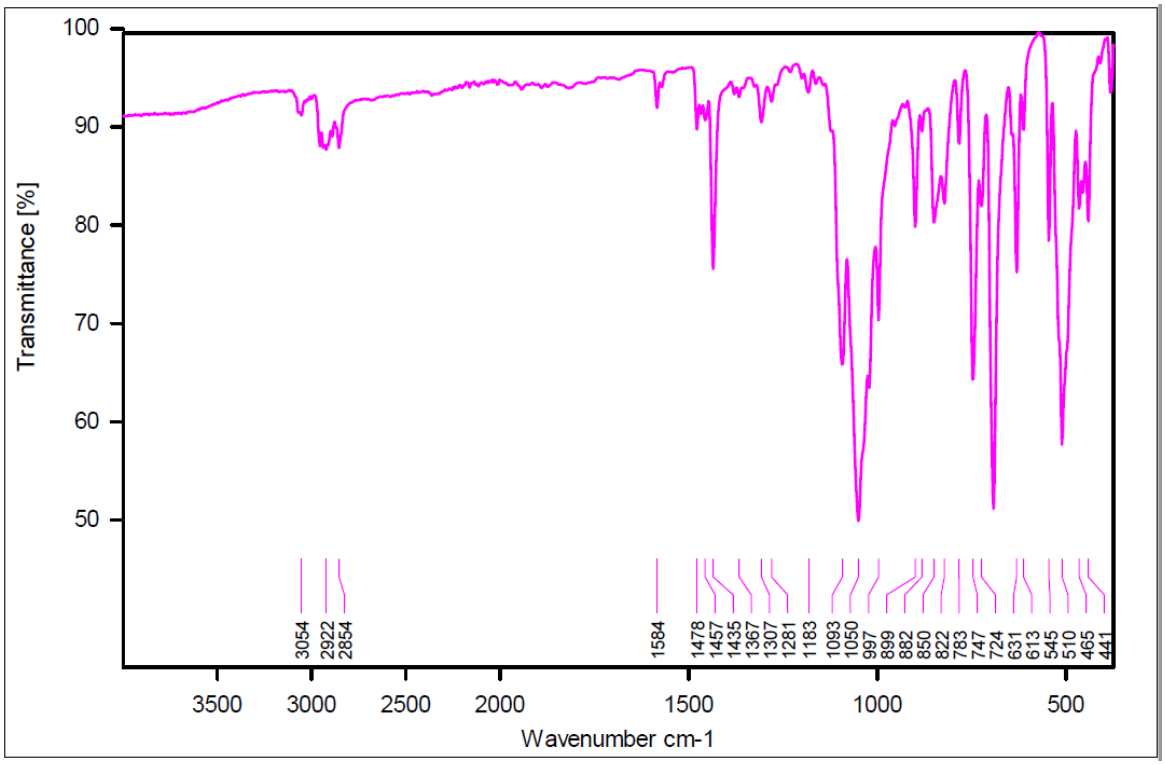

Figure S11. ATR spectrum of **1** in the solid form.

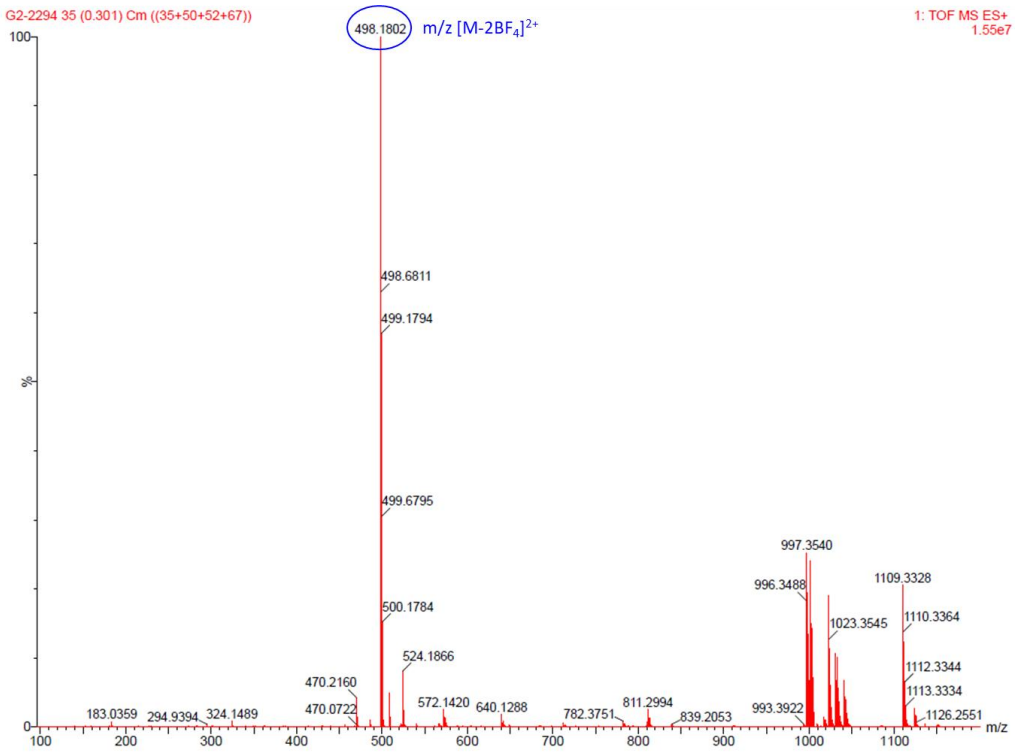

Figure S12. HR-ESI mass spectrum (positive mode) of **1**.

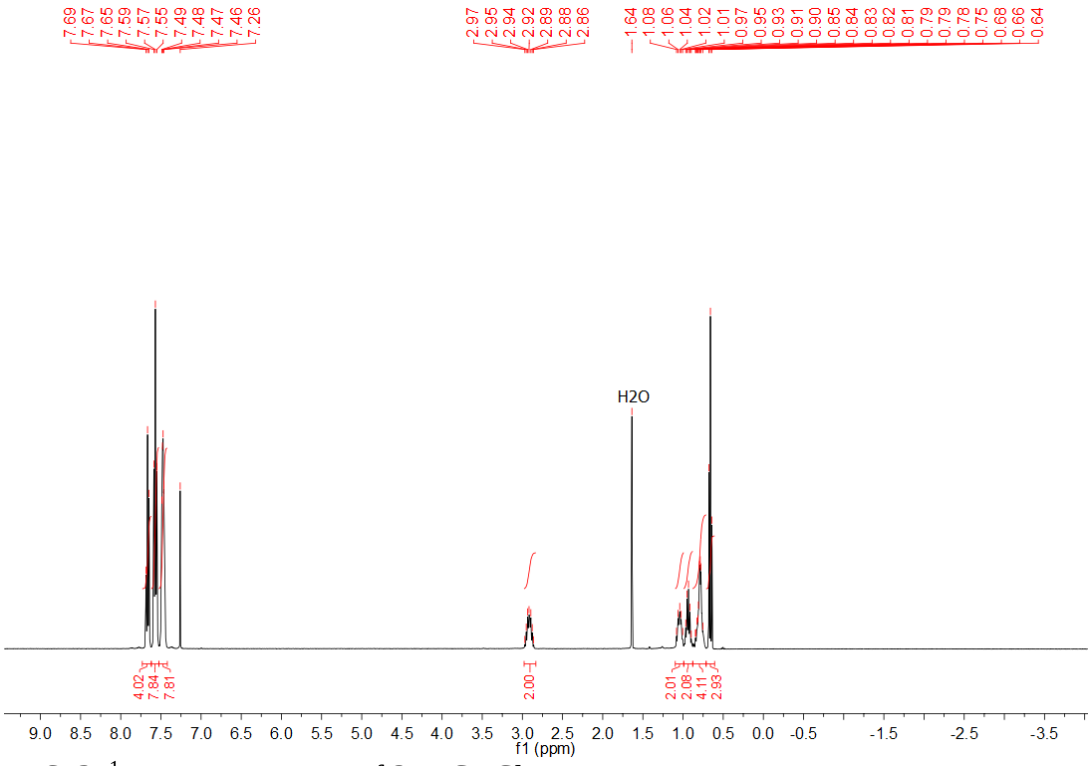

Figure S13. ^{1}H NMR spectrum of **2** in $CDCl_3$.

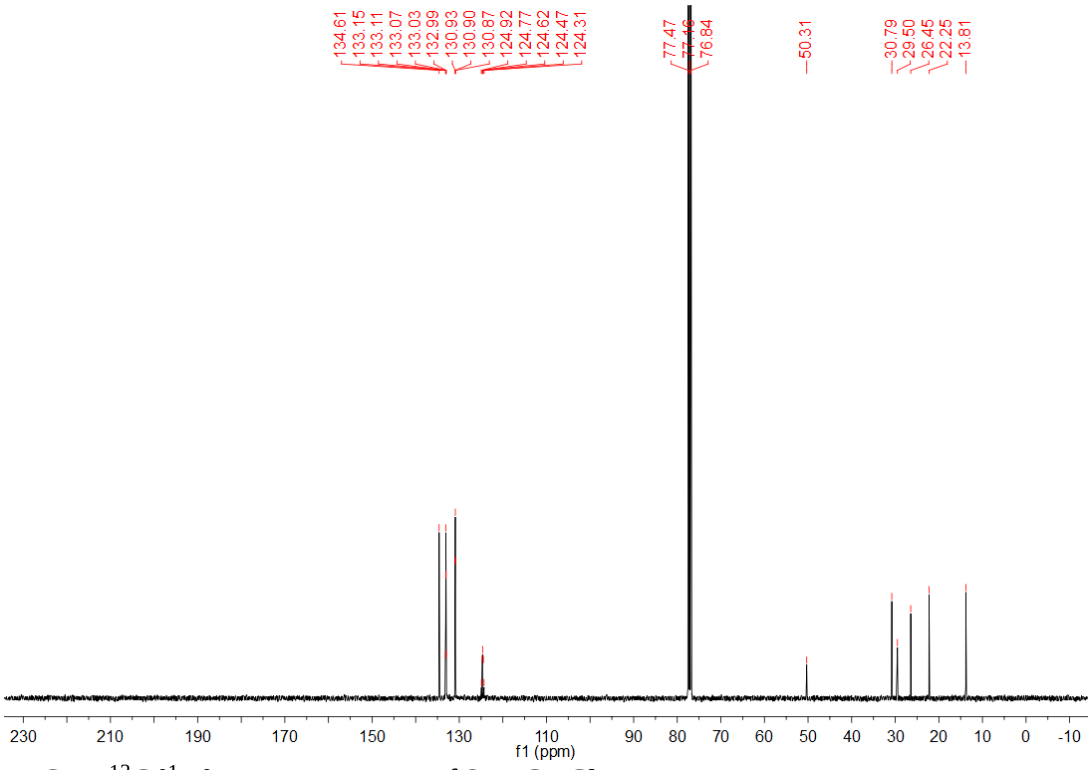

Figure S14. $^{13}C\{^{1}H\}$ NMR spectrum of **2** in $CDCl_3$.

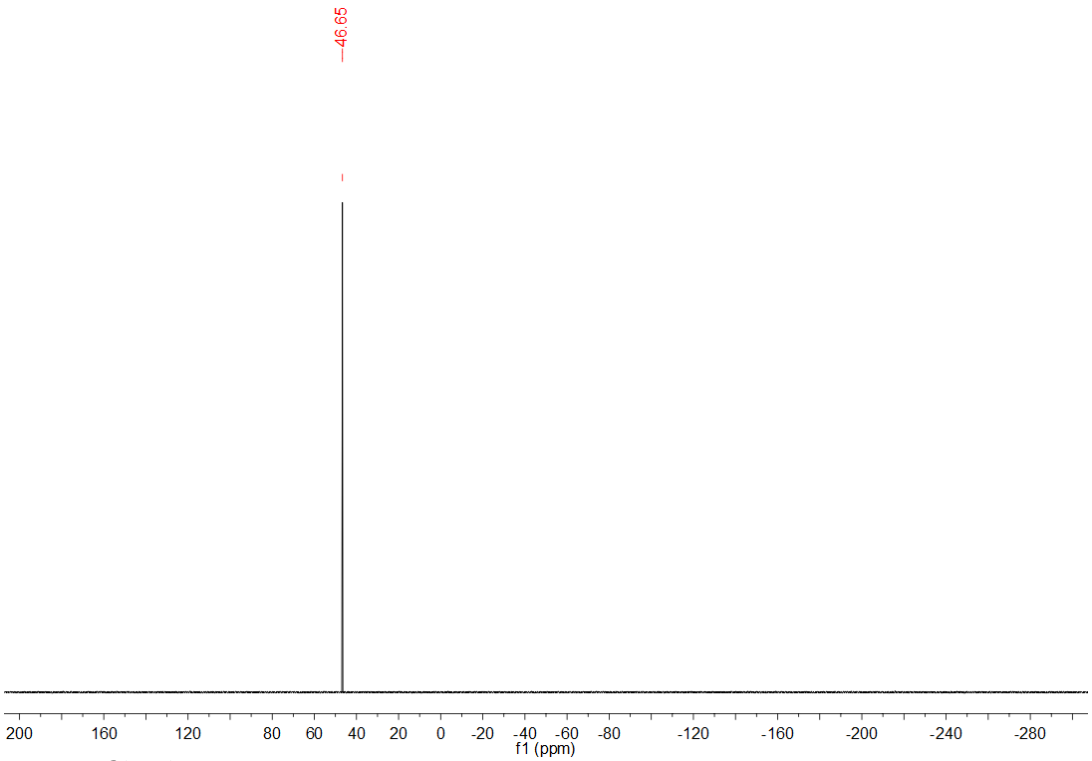

Figure S15. $^{31}P\{^{1}H\}$ NMR spectrum of **2** in $CDCl_3$.

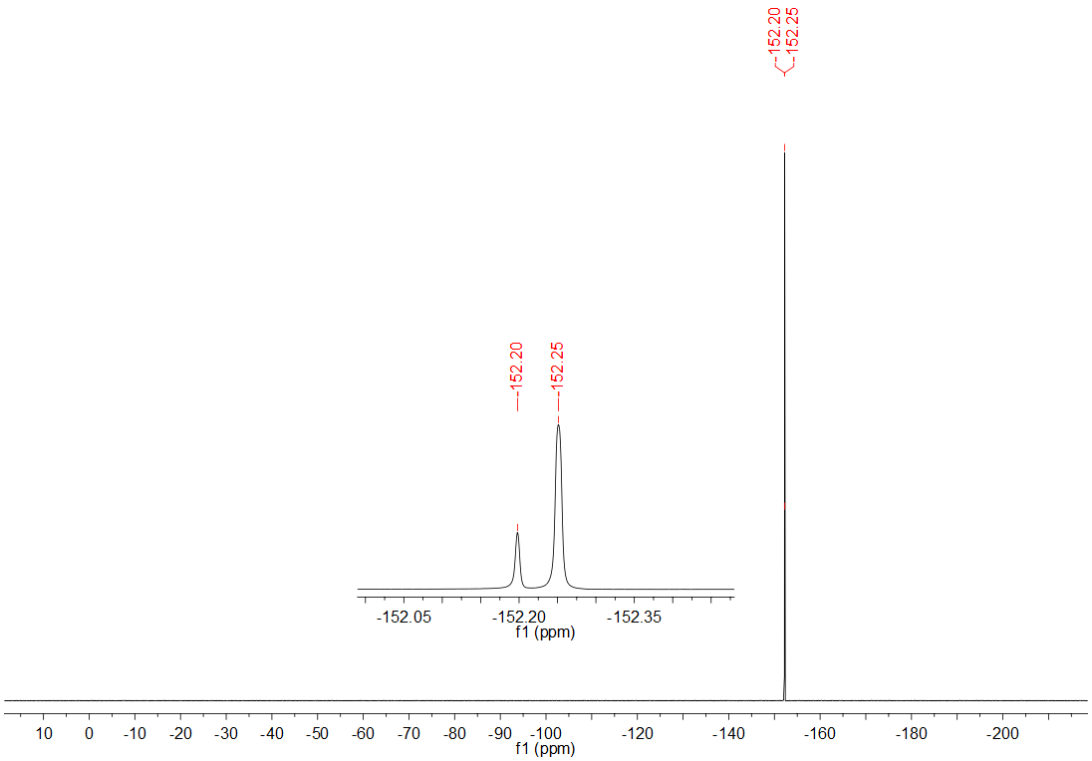

Figure S16. $^{19}F\{^{1}H\}$ NMR spectrum of **2** in $CDCl_3$.

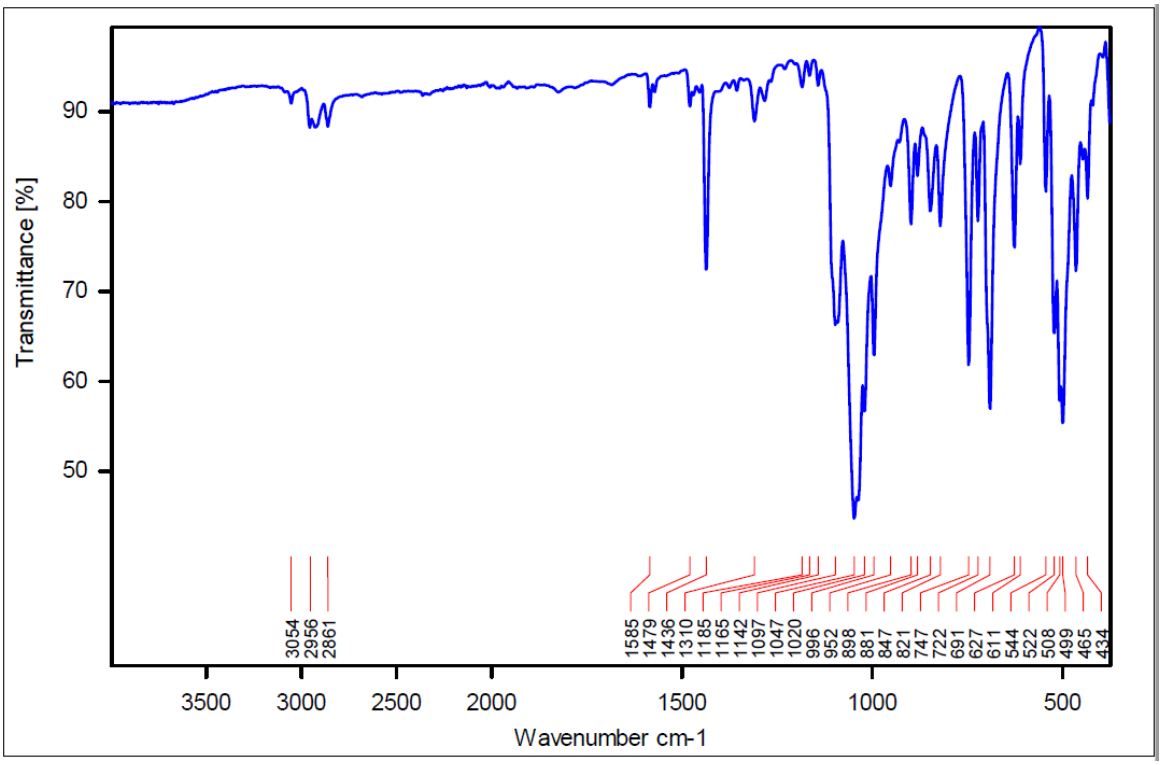

Figure S17. ATR spectrum of **2** in the solid form.

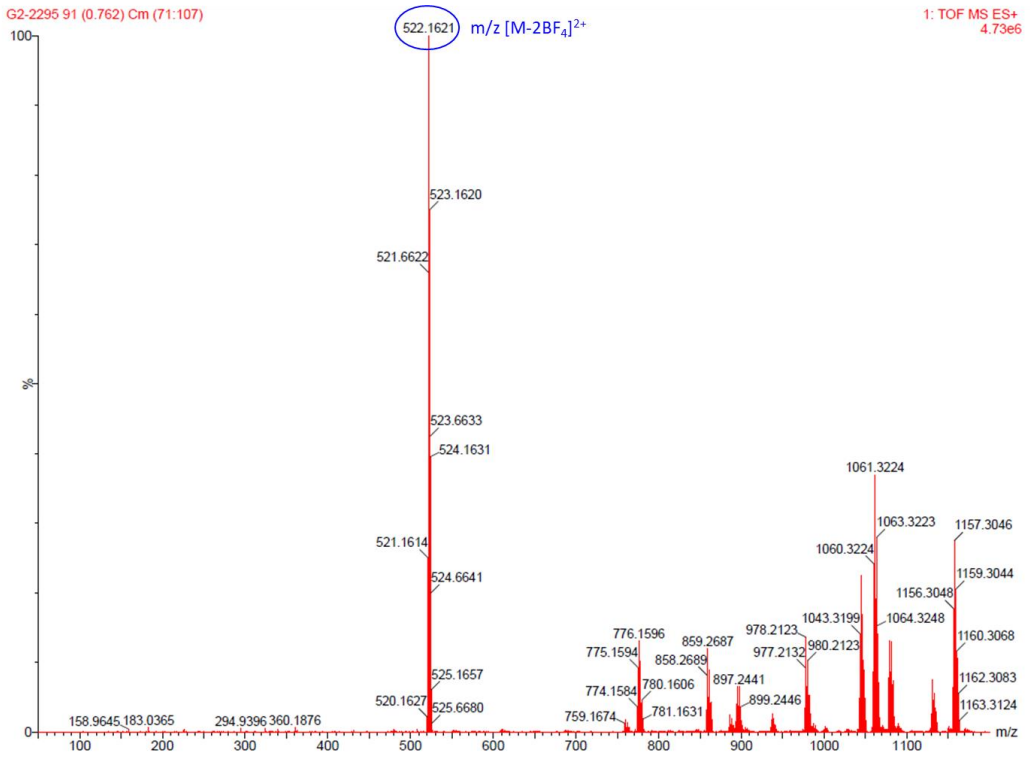

Figure S18. HR-ESI mass spectrum (positive mode) of **2**.

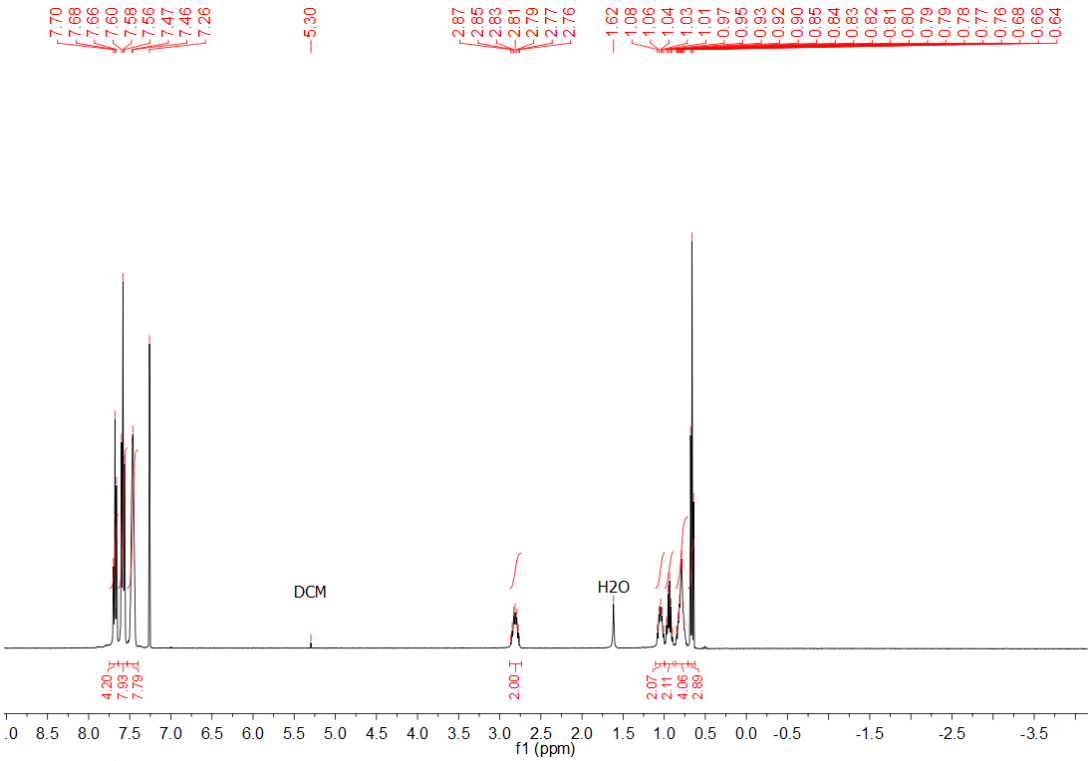

Figure S19. ^{1}H NMR spectrum of **3** in $CDCl_3$.

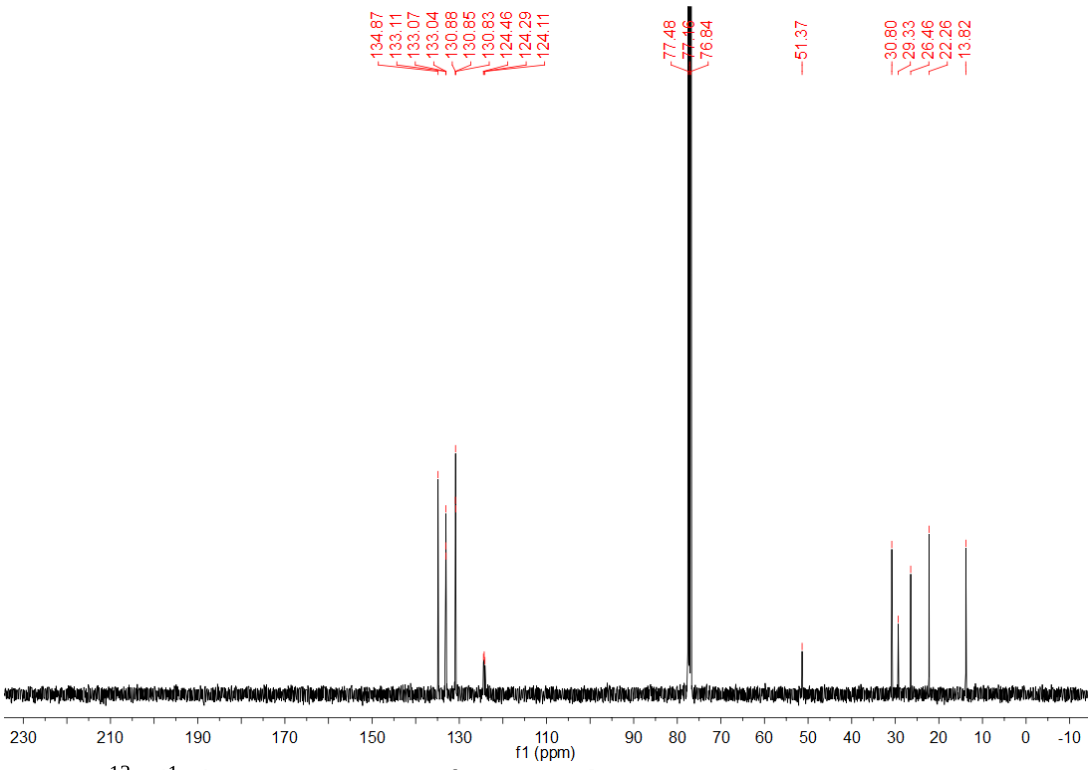

Figure S20. $^{13}C\{^{1}H\}$ NMR spectrum of **3** in $CDCl_3$.

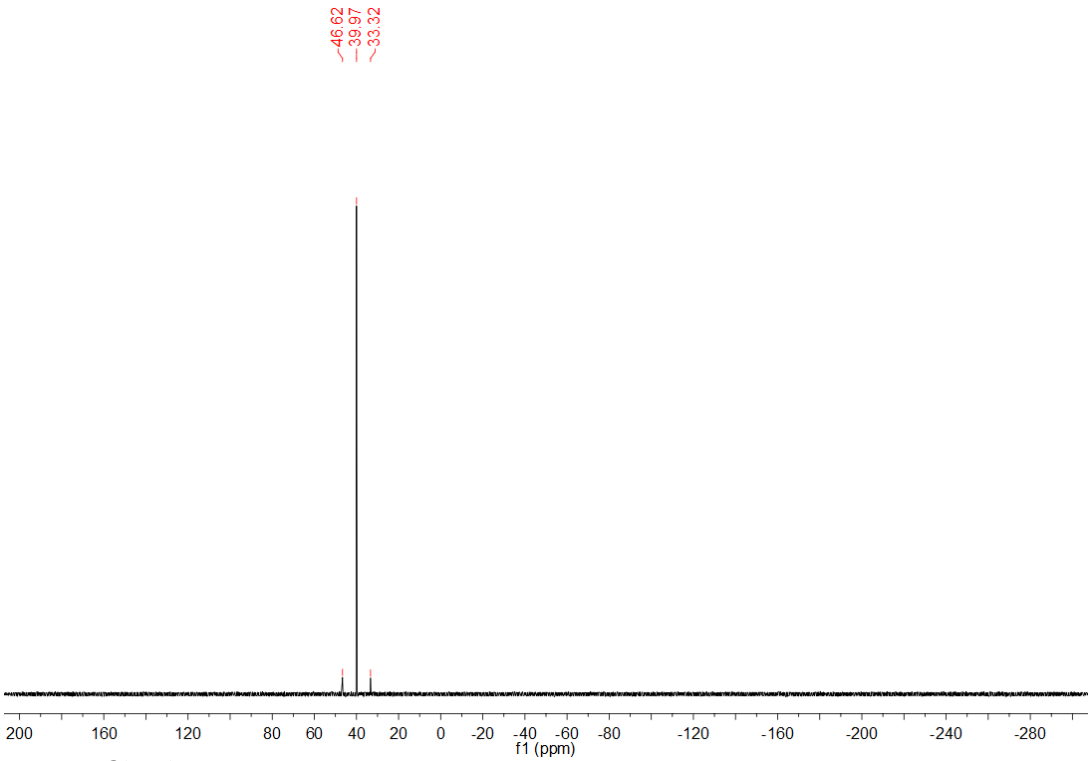

Figure S21. $^{31}P\{^{1}H\}$ NMR spectrum of **3** in $CDCl_3$.

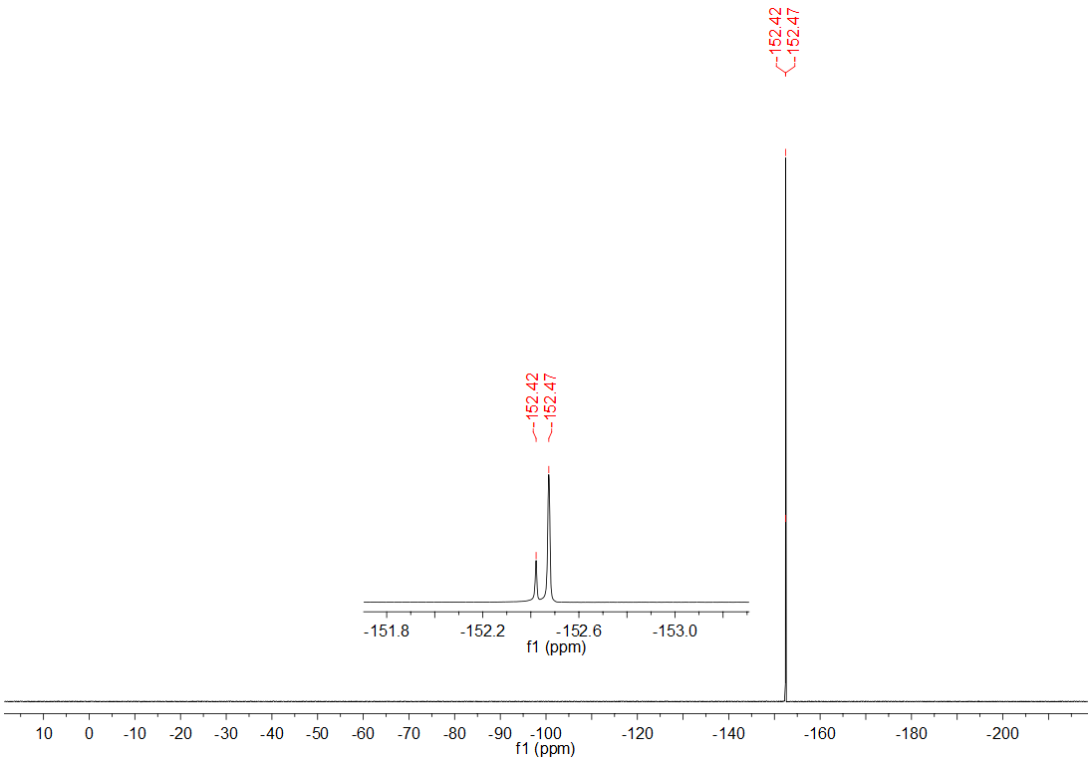

Figure S22. $^{19}F\{^{1}H\}$ NMR spectrum of **3** in $CDCl_3$.

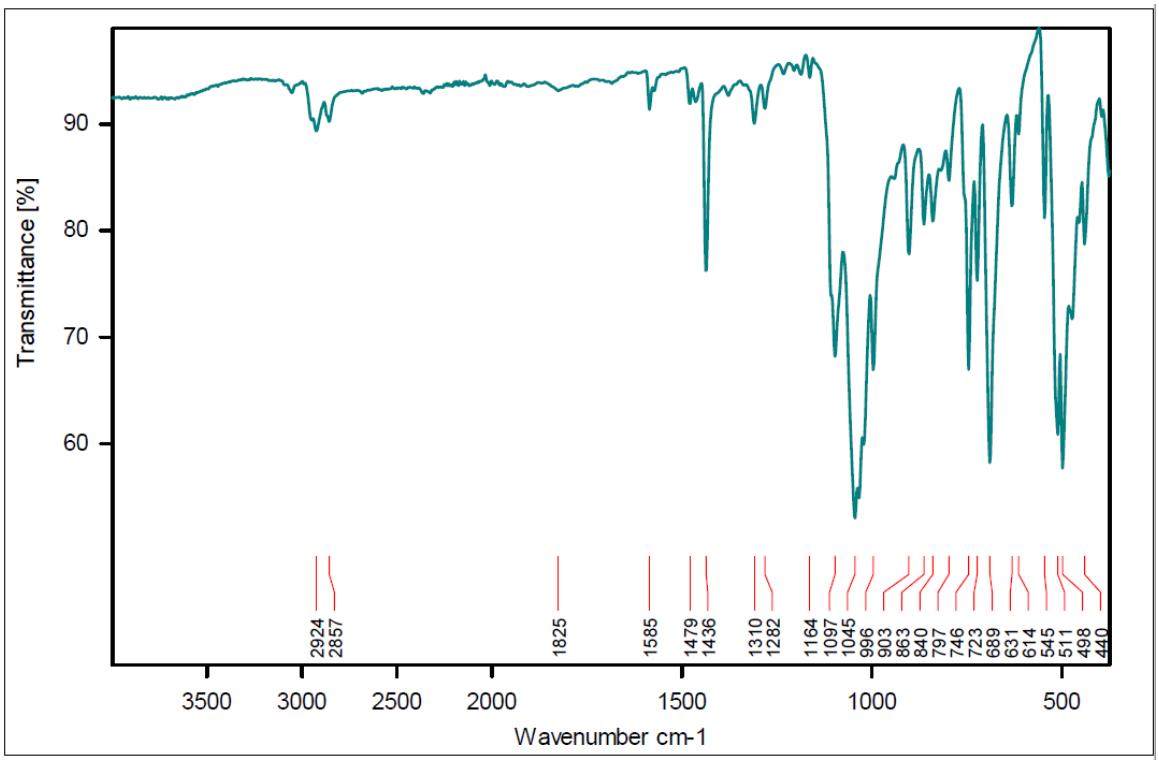

Figure S23. ATR spectrum of **3** in the solid form.

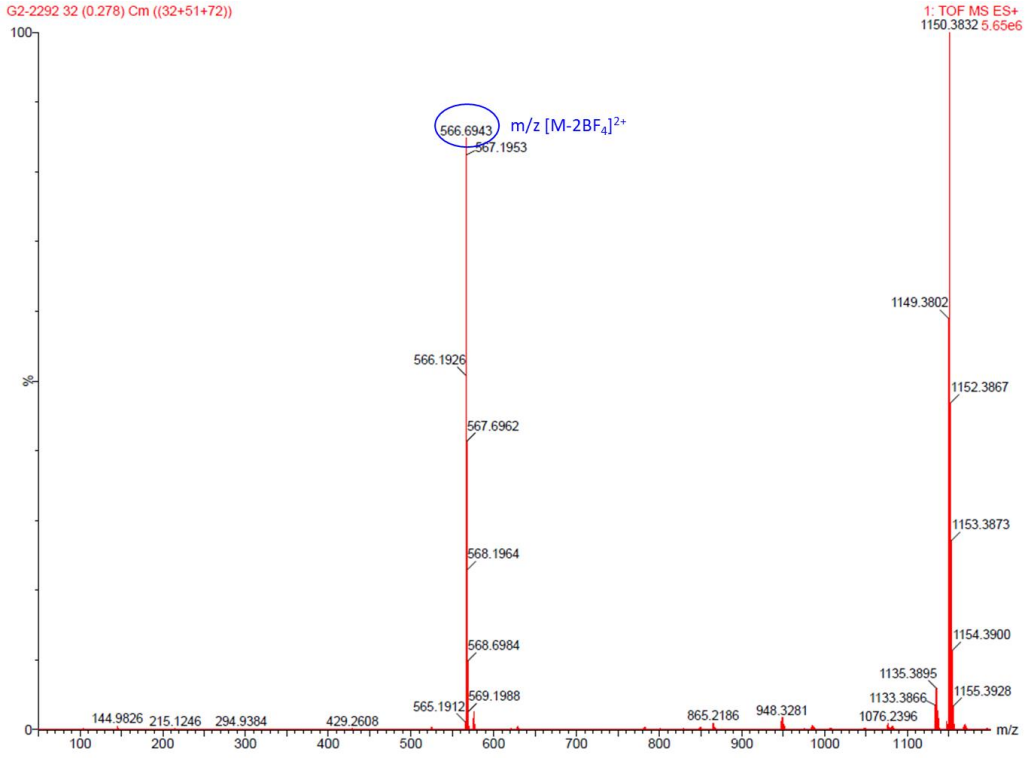

Figure S24. HR-ESI mass spectrum (positive mode) of **3**.

Table S1. Crystallographic data for complexes **1**-**3**.

Metal complex	**1**	**2**	**3**
CCDC No.	2035448	2035447	2035446
formula	$C_{60}H_{66}N_2P_4B_2F_8Ni$ •$4CH_2Cl_2$	$C_{60}H_{66}B_2N_2F_8P_4Pd$	$C_{60}H_{66}B_2N_2F_8P_4Pt$
Fw	1511.06	1219.04	1307.73
Crystal system	monoclinic	monoclinic	triclinic
Space group	*C2/c*	*$P2_1/n$*	*P-1*
a, Å	26.157(11)	11.261(3)	10.428(3)
b, Å	13.807(6)	18.581(4)	11.850(3)
c, Å	20.261(8)	14.211(3)	23.584(6)
α, deg.	90	90	77.044(4)
β, deg.	97.582(9)	99.736(4)	81.378(4)
γ, deg.	90	90	82.984(5)
V, $Å^3$	7253(5)	2930.7(11)	2796.2(12)
Z	4	2	2
D_{calcd}, Mg/m^3	1.384	1.381	1.553
2*θ* / deg.	3.142 to 52	3.642 to 51.998	1.786 to 51.998
Reflections collected	18129	22267	10881
Independent reflections	6913	5751	10881
Goodness-of-fit on F^2	0.940	1.008	1.051
R_1, wR_2 [$I \geq 2\sigma(I)$]	0.0752, 0.1674	0.0418, 0.0902	0.0599, 0.1105
R_1, wR_2 [all data]	0.1398, 0.1935	0.0563, 0.0945	0.0868, 0.1181

Table S2. Selected bond lengths (Å) and angles (°) for complex **1**.

Ni(1)-P(1)	2.1715(13)	P(1)-C(1)	1.800(5)
Ni(1)-P(2)	2.1822(15)	P(1)-C(7)	1.790(5)
N(1)-P(1)	1.693(4)	P(2)-C(13)	1.796(5)
N(1)-P(2)	1.699(4)	P(2)-C(19)	1.798(5)
N(1)-C(25)	1.471(6)		
P(1)-Ni(1)-P(2)	73.32(5)	C(1)-P(1)-Ni(1)	118.43(16)
P(1)-Ni(1)-P(1)^{1}	180.0	C(7)-P(1)-Ni(1)	117.08(16)
P(1)-Ni(1)-P(2)^{1}	106.68(5)	C(13)-P(2)-Ni(1)	117.82(16)
N(1)-P(1)-Ni(1)	92.98(14)	C(19)-P(2)-Ni(1)	119.47(17)
N(1)-P(2)-Ni(1)	92.46(14)	P(1)-N(1)-P(2)	100.1(2)

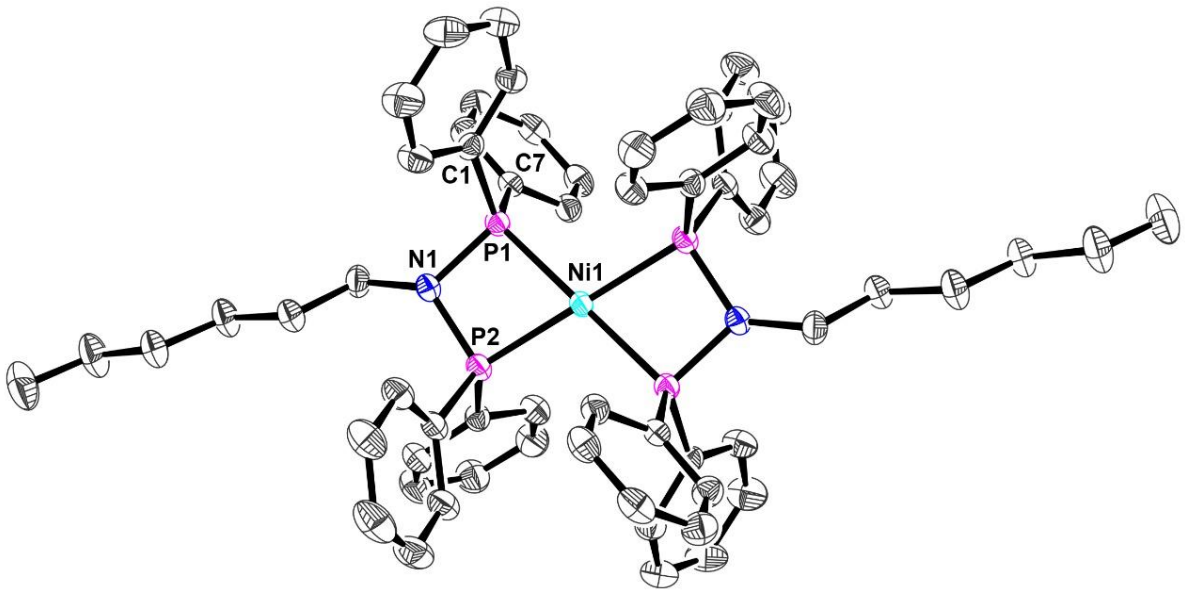

Table S3. Selected bond lengths (Å) and angles (°) for complex **2**.

Pd(1)-P(1)	2.2962(8)	P(1)-C(1)	1.799(3)
Pd(1)-P(2)	2.3172(7)	P(1)-C(7)	1.802(3)
N(1)-P(1)	1.699(2)	P(2)-C(13)	1.808(3)
N(1)-P(2)	1.719(2)	P(2)-C(19)	1.803(3)
N(1)-C(25)	1.487(3)		
P(1)-Pd(1)-P(2)	69.32(2)	C(1)-P(1)-Pd(1)	118.35(9)
P(1)-Pd(1)-P(1)^{1}	180.0	C(7)-P(1)-Pd(1)	117.16(9)
P(1)-Pd(1)-P(2)^{1}	110.68(2)	C(13)-P(2)-Pd(1)	115.81(9)
N(1)-P(1)-Pd(1)	92.63(7)	C(19)-P(2)-Pd(1)	121.34(9)
N(1)-P(2)-Pd(1)	91.39(8)	P(1)-N(1)-P(2)	100.26(11)

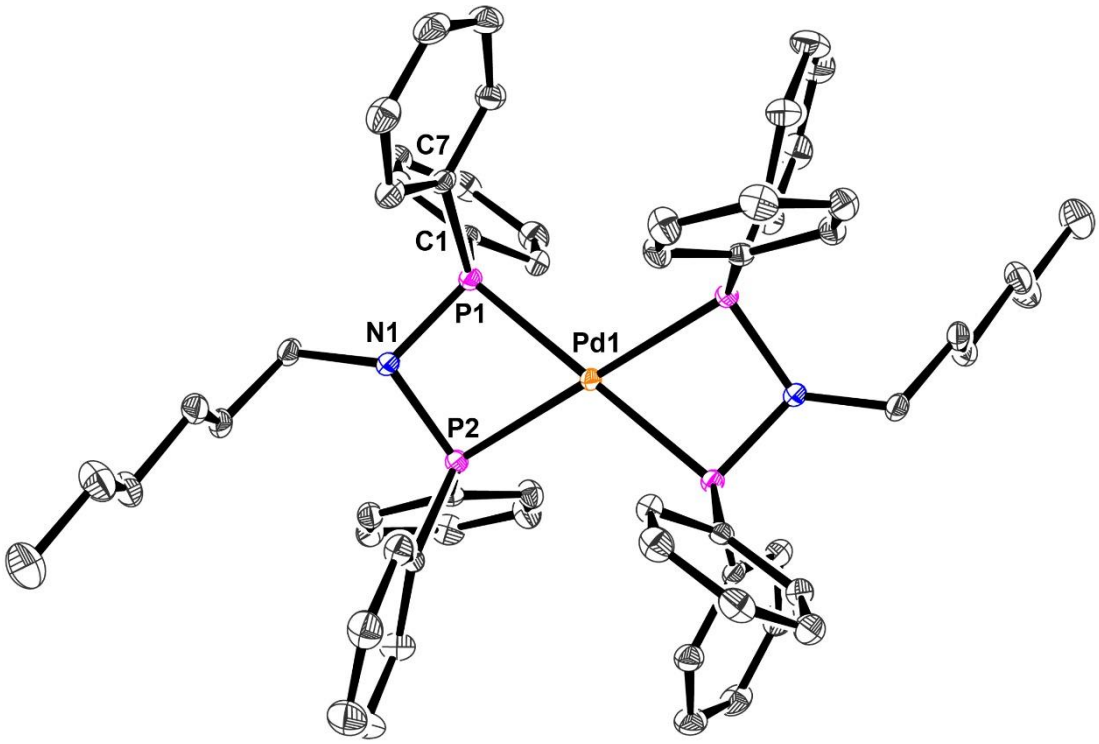

Table S4. Selected bond lengths (Å) and angles (°) for complex **3**.

Pt(1)-P(1)	2.3020(19)	P(1)-C(1)	1.803(8)
Pt(1)-P(2)	2.2957(19)	P(1)-C(7)	1.795(8)
N(1)-P(1)	1.710(6)	P(2)-C(13)	1.794(7)
N(1)-P(2)	1.681(6)	P(2)-C(19)	1.793(7)
N(1)-C(25)	1.467(9)		
P(1)-Pt(1)-P(2)	69.83(7)	C(1)-P(1)-Pt(1)	118.5(2)
P(1)-Pt(1)-P(1)^{1}	180.0	C(7)-P(1)-Pt(1)	118.7(3)
P(1)-Pt(1)-P(2)^{1}	110.17(7)	C(13)-P(2)-Pt(1)	120.1(3)
N(1)-P(1)-Pt(1)	92.9(2)	C(19)-P(2)-Pt(1)	113.9(2)
N(1)-P(2)-Pt(1)	94.0(2)	P(1)-N(1)-P(2)	101.8(3)

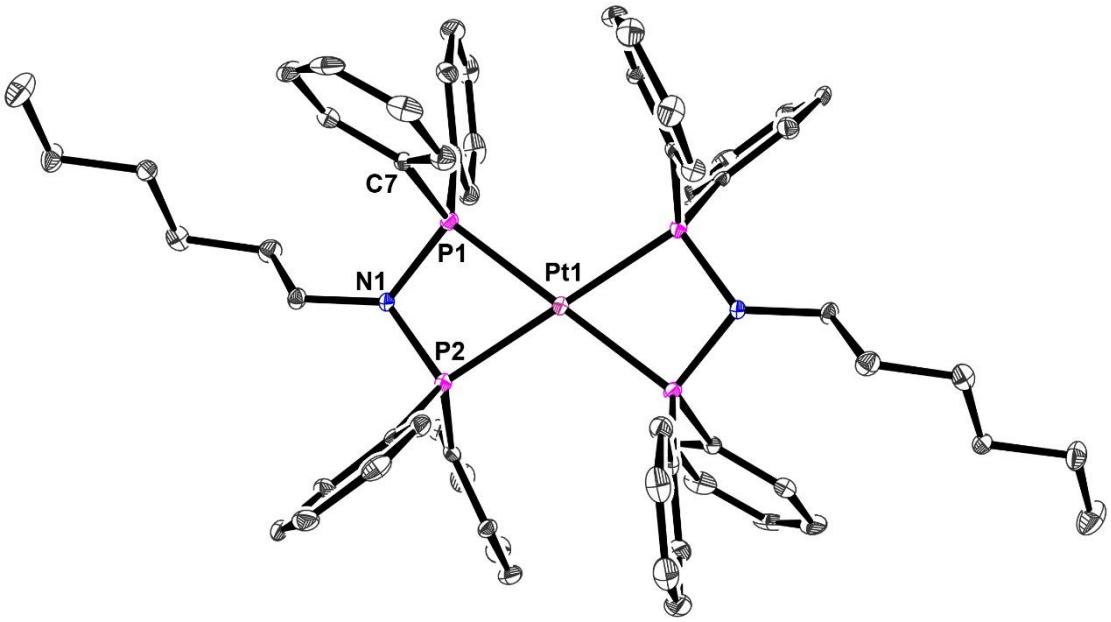

Table S5. Experimentally determined LogP values for **1-3**.

Metal complex	LogP
1	0.15
2	0.36
3	0.32

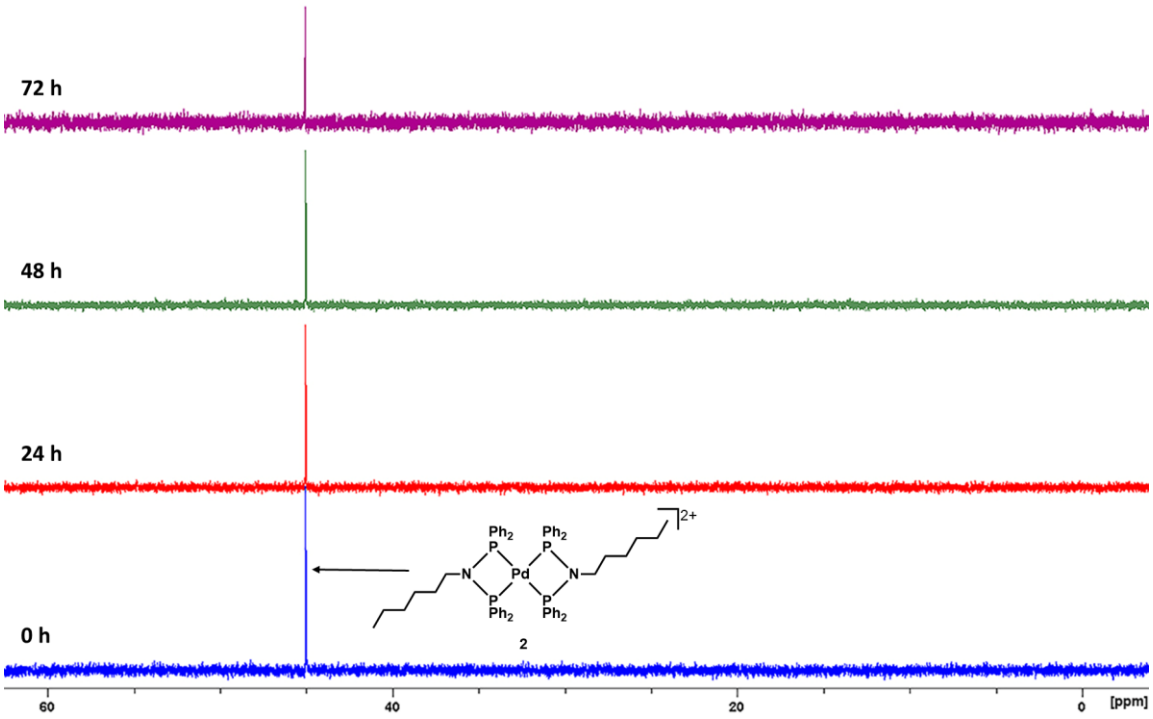

Figure S25. $^{31}P\{^{1}H\}$ NMR spectra of **2** (1 mM) in DMSO-d_6 over the course of 72 h.

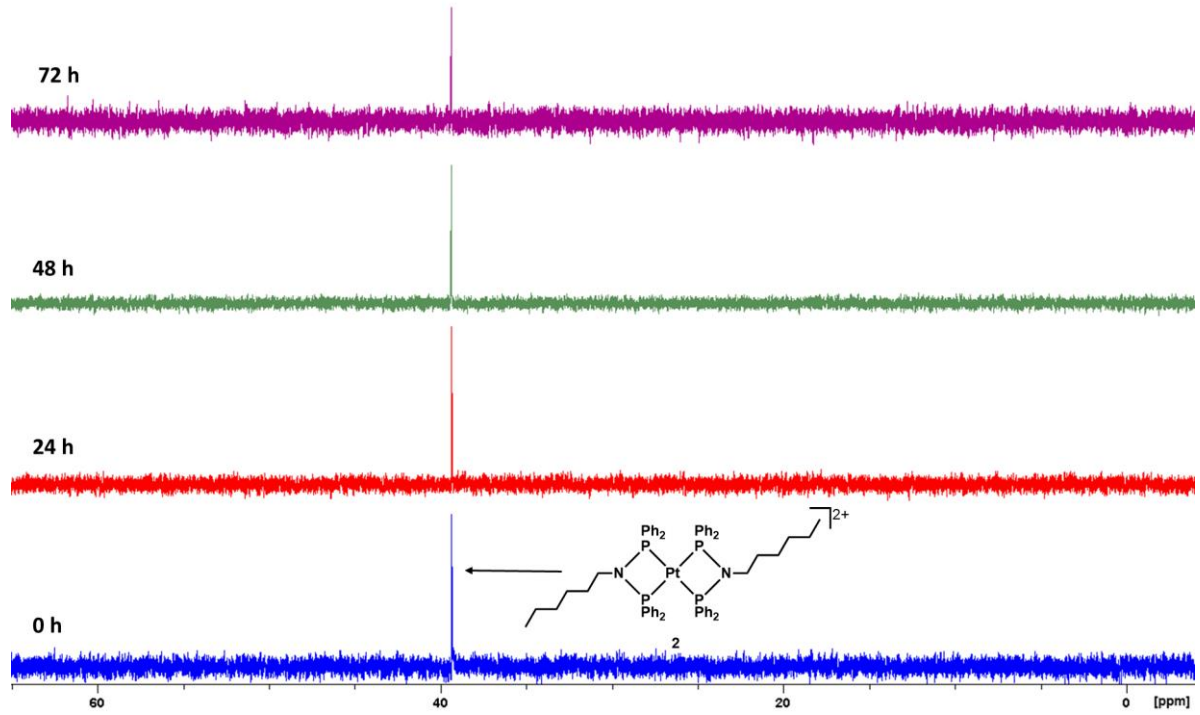

Figure S26. $^{31}P\{^{1}H\}$ NMR spectra of **3** (1 mM) in DMSO-d_6 over the course of 72 h.

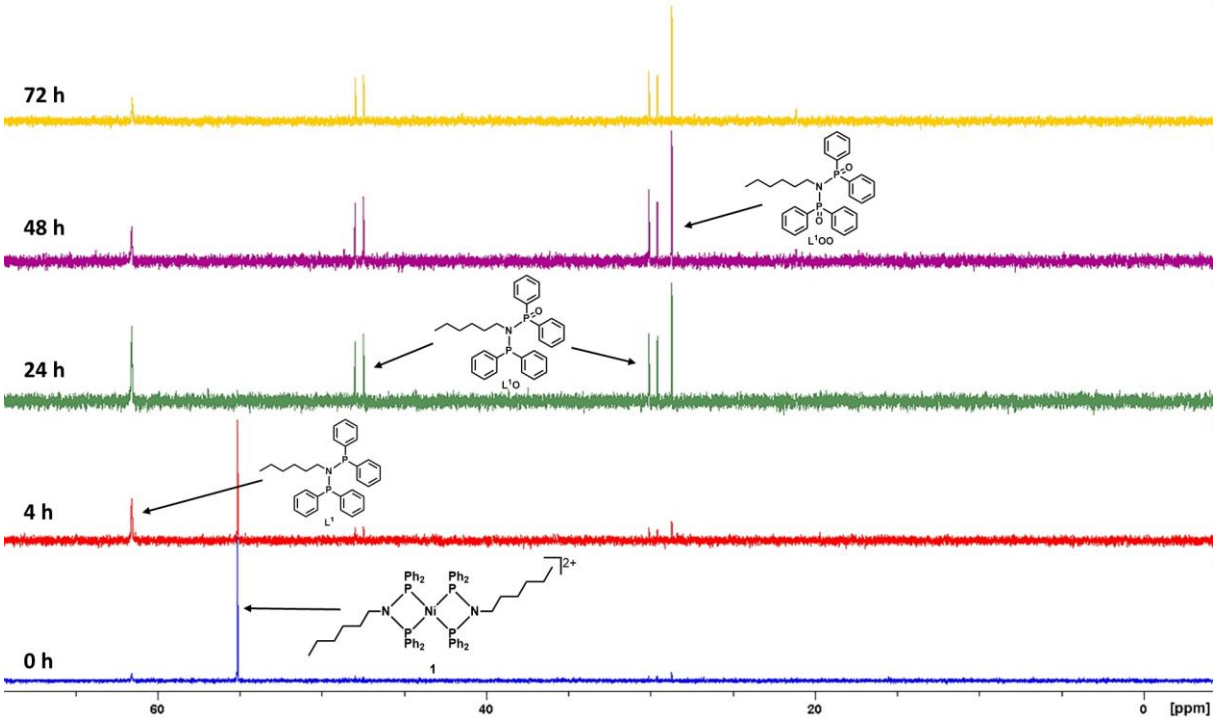

Figure S27. $^{31}P\{^{1}H\}$ NMR spectra of **1** (1 mM) in DMSO-d_6 over the course of 72 h.

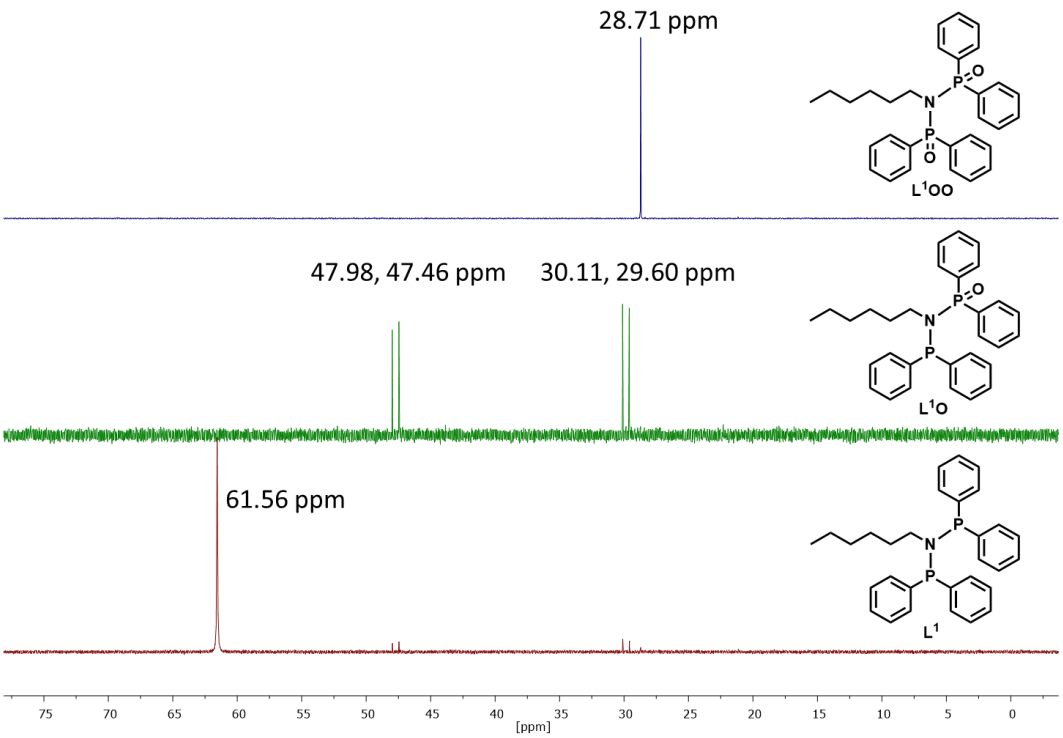

Figure S28. ^{1}H NMR spectra of **L^{1}**, **L^{1}O**, and **L^{1}OO** in DMSO-d_6.

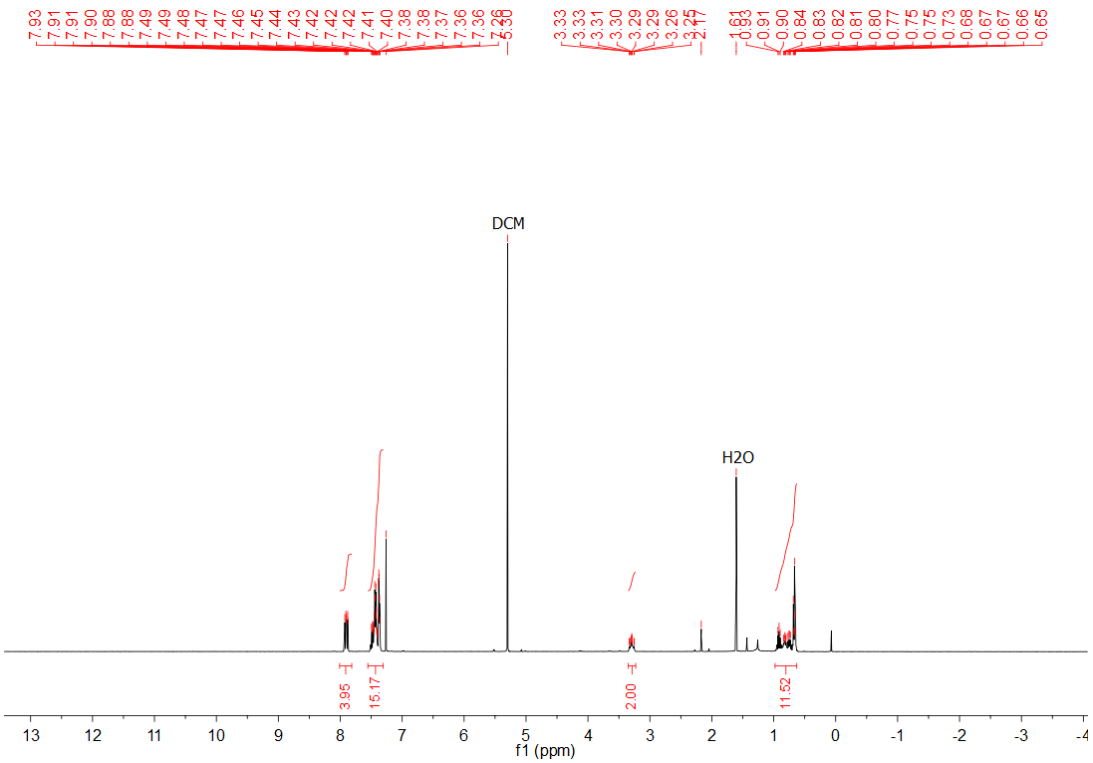

Figure S29. ^{1}H NMR spectrum of **L^{1}O** in $CDCl_3$.

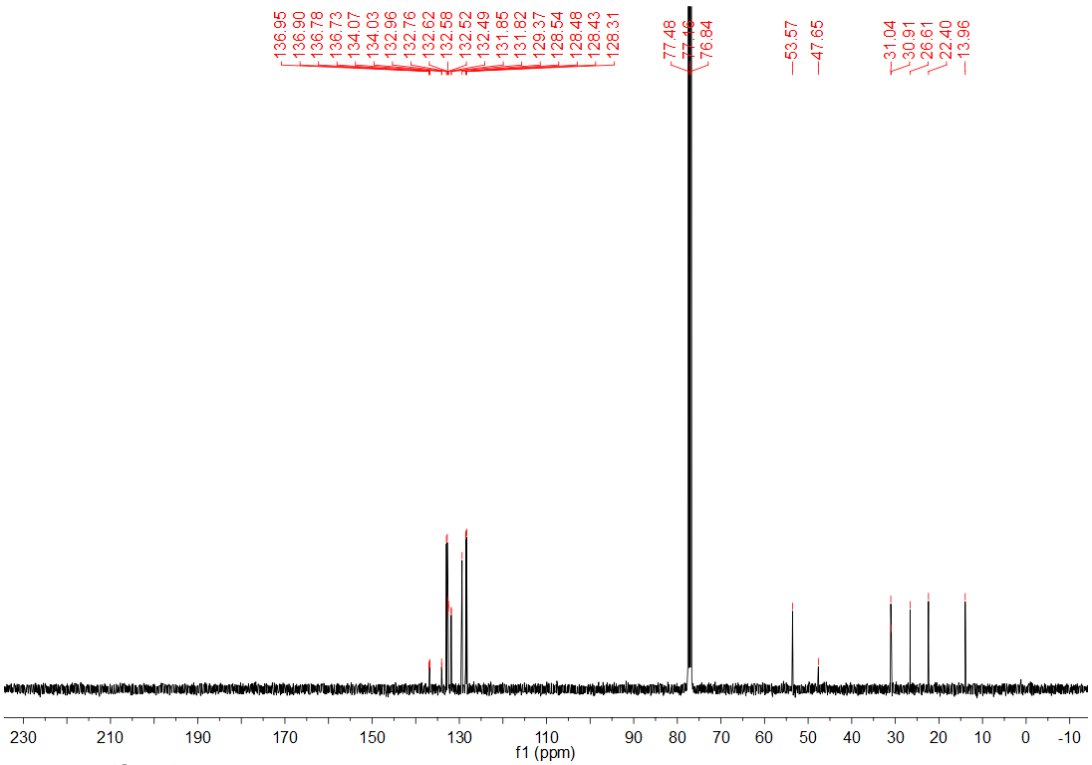

Figure S30. $^{13}C\{^{1}H\}$ NMR spectrum of **L^{1}O** in $CDCl_3$.

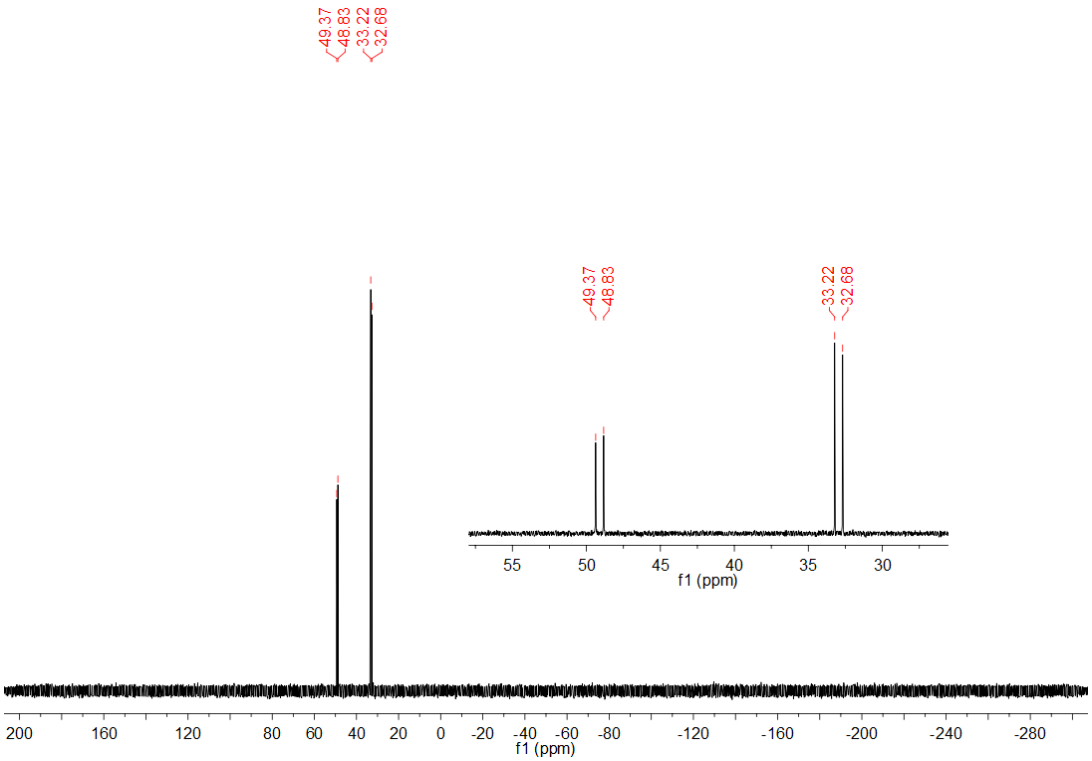

Figure S31. $^{31}P\{^{1}H\}$ NMR spectrum of **L^{1}O** in $CDCl_3$.

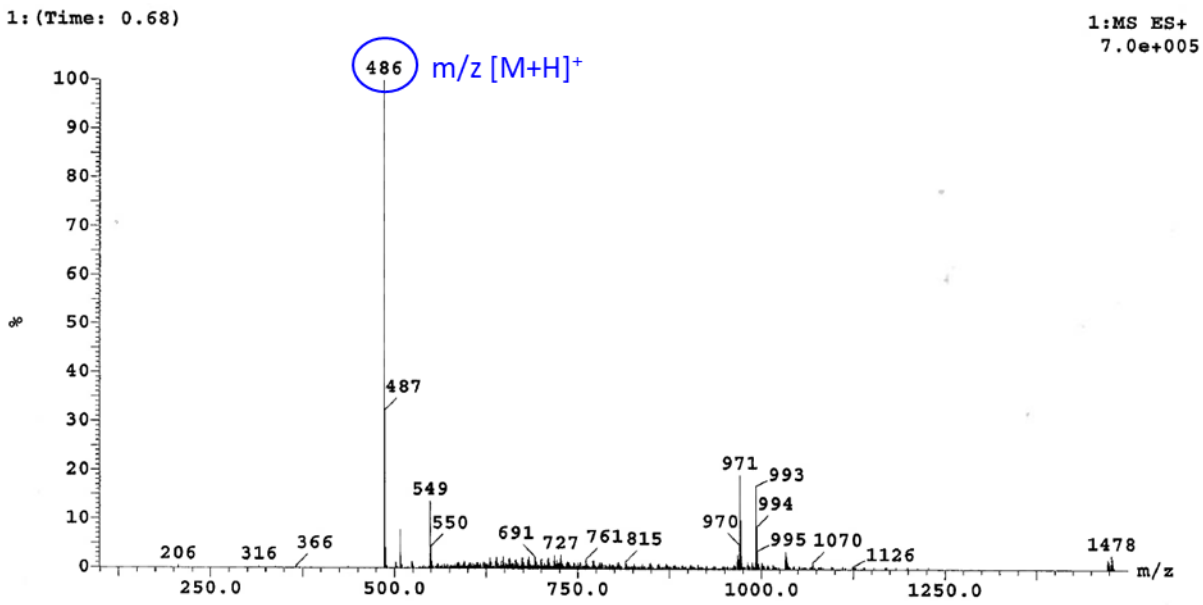

Figure S32. ESI mass spectrum (positive mode) of **L^{1}O**.

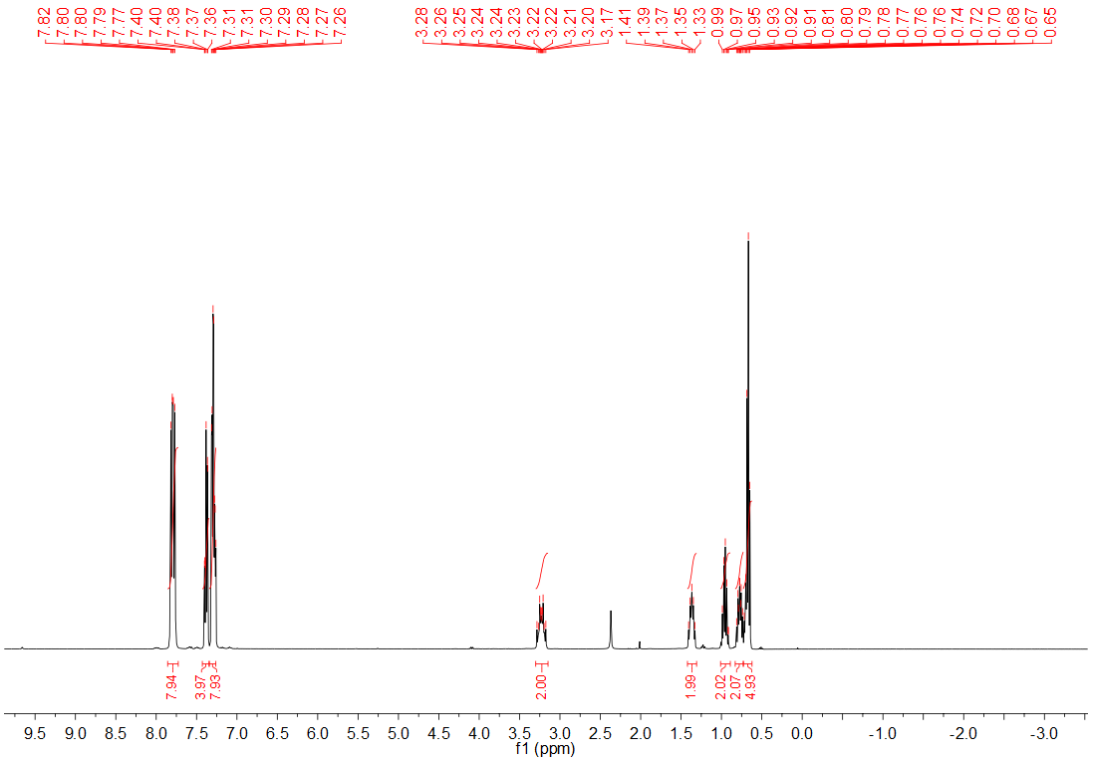

Figure S33. ^{1}H NMR spectrum of **L^{1}OO** in $CDCl_3$.

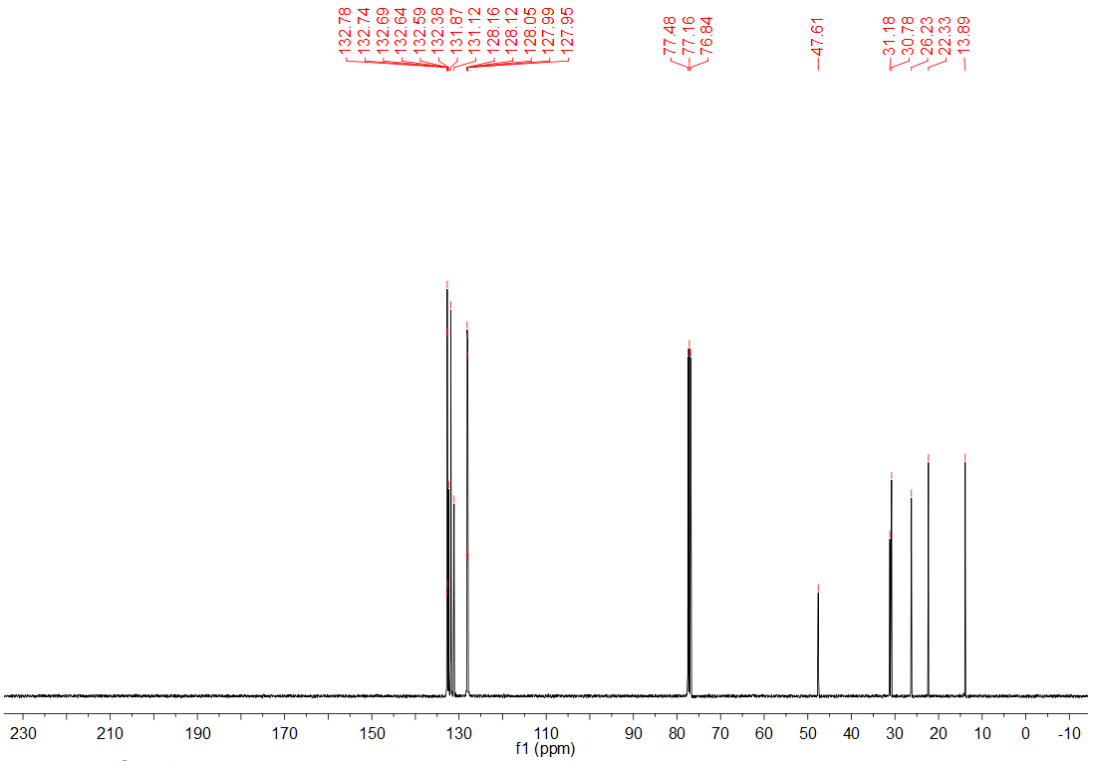

Figure S34. $^{13}C\{^{1}H\}$ NMR spectrum of **L^{1}OO** in $CDCl_3$.

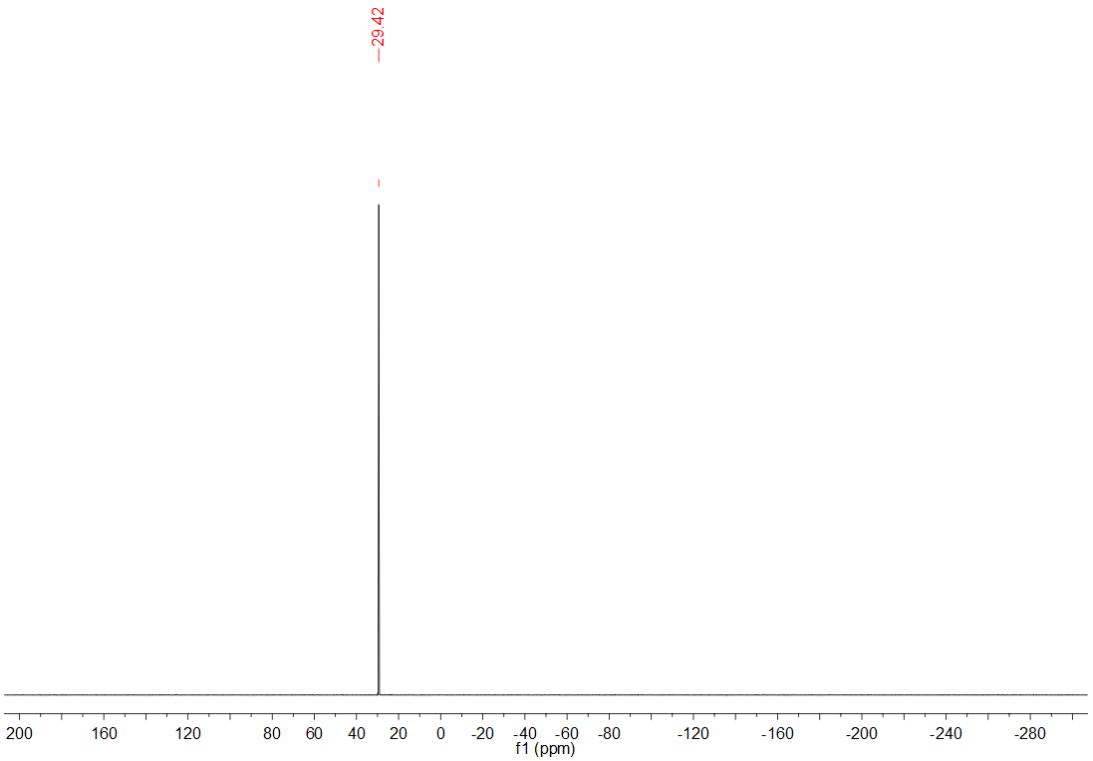

Figure S35. $^{31}P\{^{1}H\}$ NMR spectrum of **L^{1}OO** in $CDCl_3$.

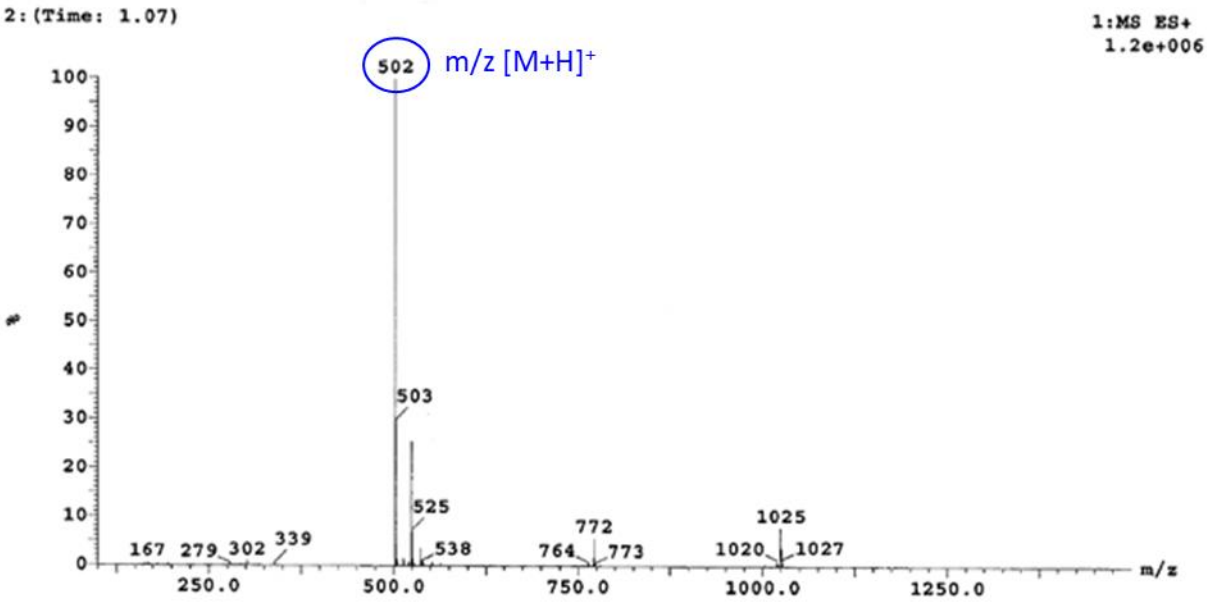

Figure S36. ESI mass spectrum (positive mode) of **L^{1}OO**.

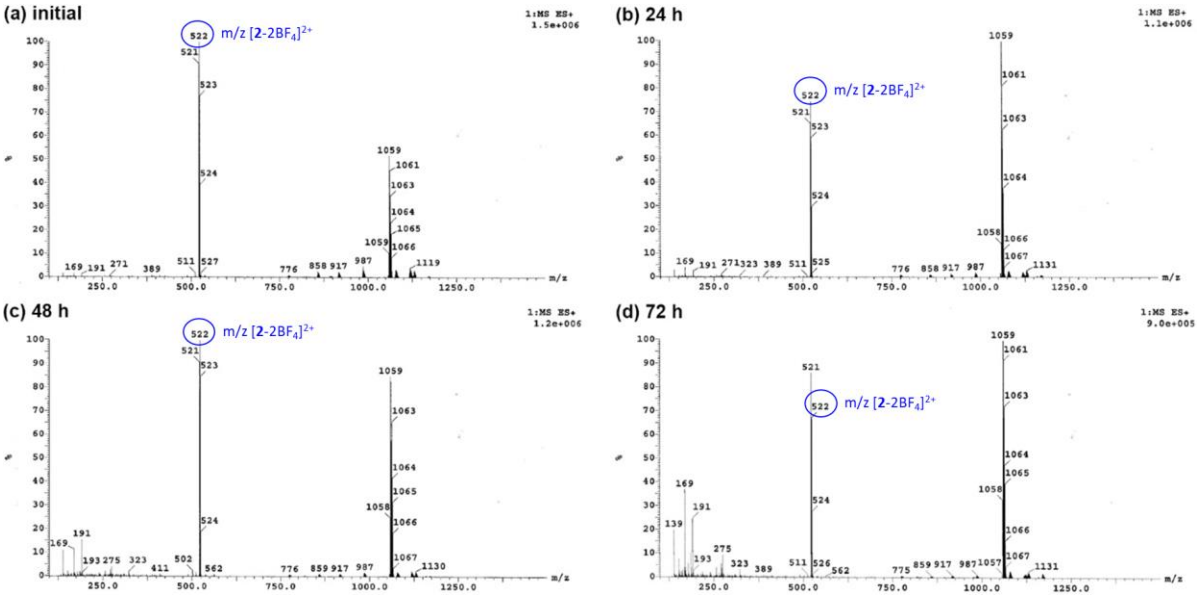

Figure S37. ESI mass spectra of **2** in H_2O:DMSO (200:1) over the course of 72 h at 37 ^oC.

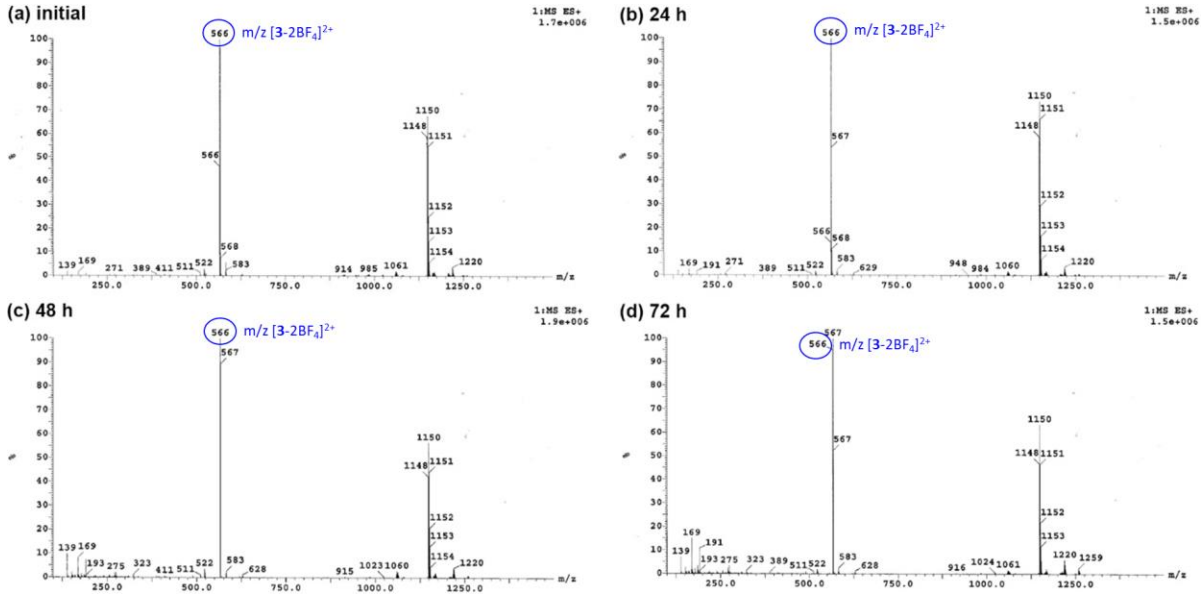

Figure S38. ESI mass spectra of **3** in H_2O:DMSO (200:1) over the course of 72 h at 37 ^oC.

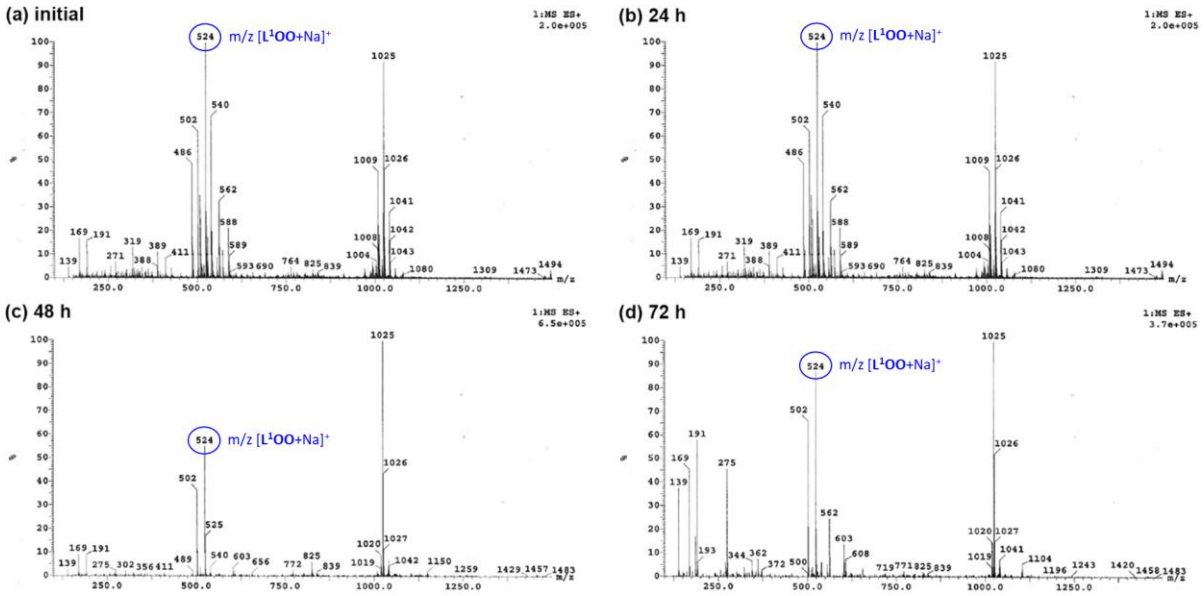

Figure S39. ESI mass spectra of **1** in H_2O:DMSO (200:1) over the course of 72 h at 37 ^oC.

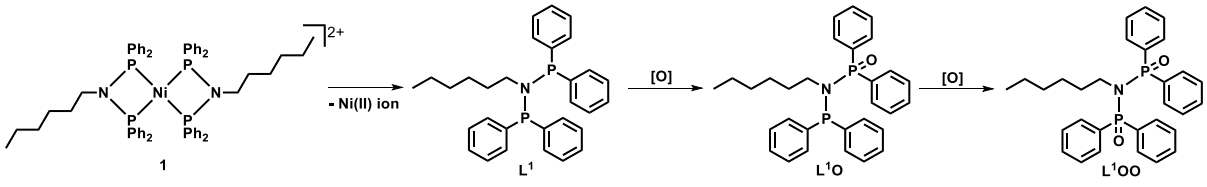

Figure S40. Possible decomposition pathway of **1** in solution.

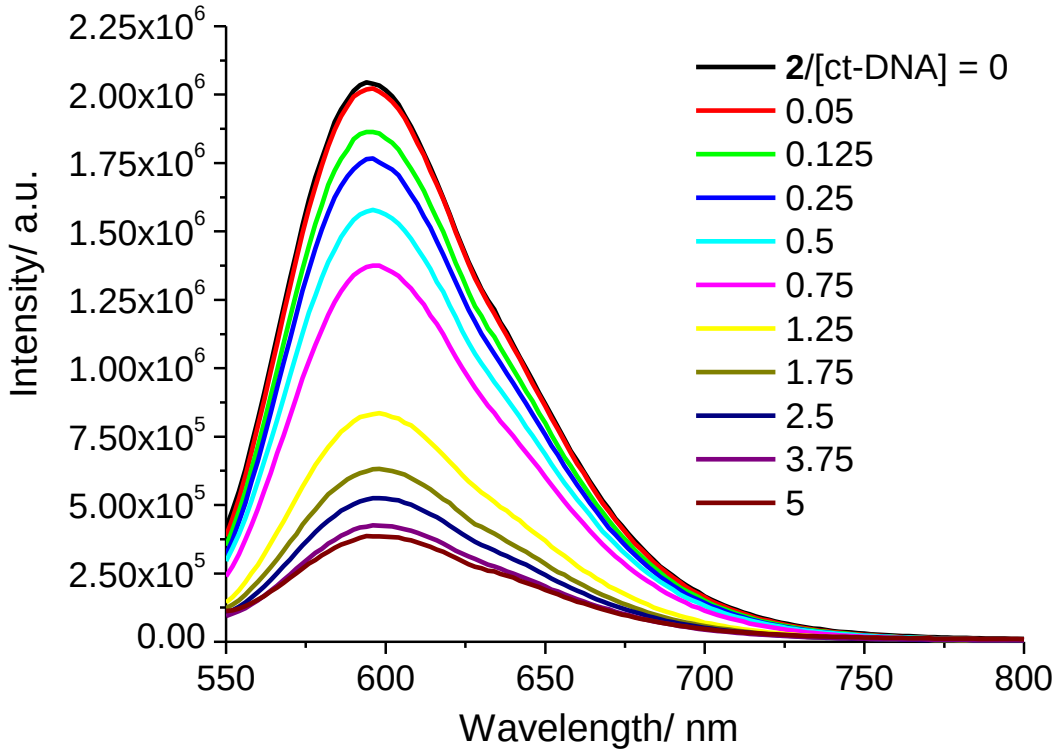

Figure S41. Representative emission spectra for ethidium bromide (1 μM) bound to ct-DNA (1:20 ratio) upon addition of aliquots of **2**.

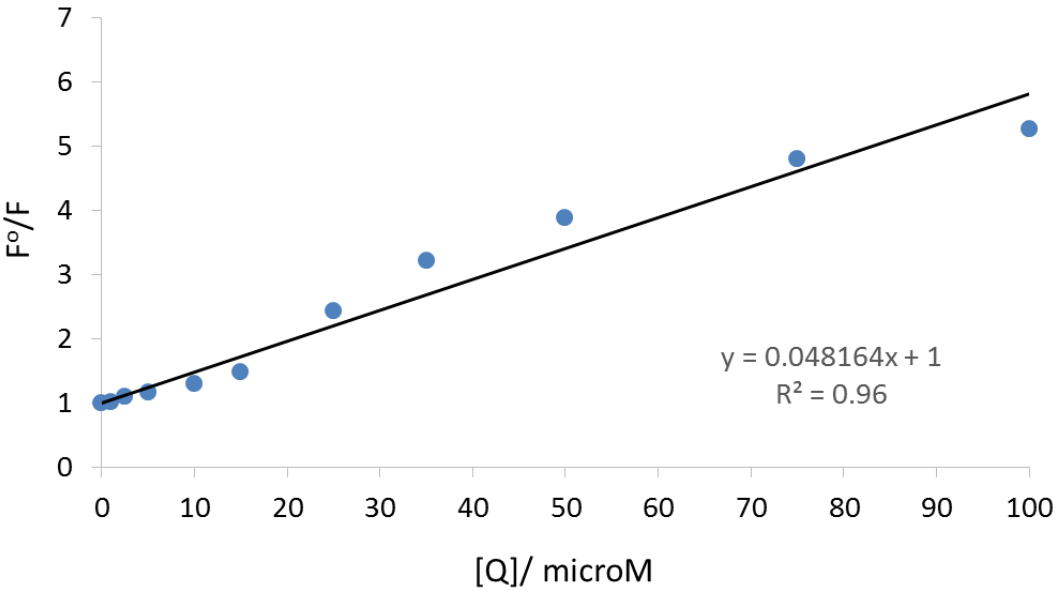

Figure S42. Representative F^o/F versus [Q] plot corresponding to the emission spectra for ethidium bromide (1 μM) bound to ct-DNA (1:20 ratio) upon addition of aliquots of **2**.

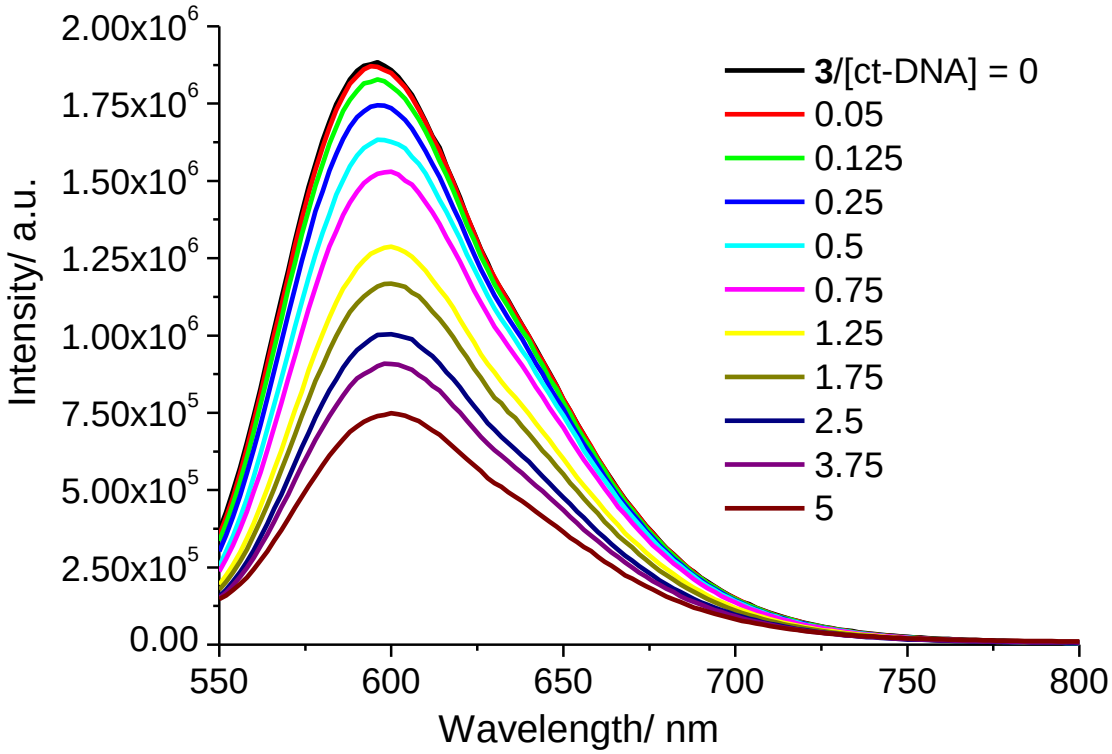

Figure S43. Representative emission spectra for ethidium bromide (1 μM) bound to ct-DNA (1:20 ratio) upon addition of aliquots of **3**.

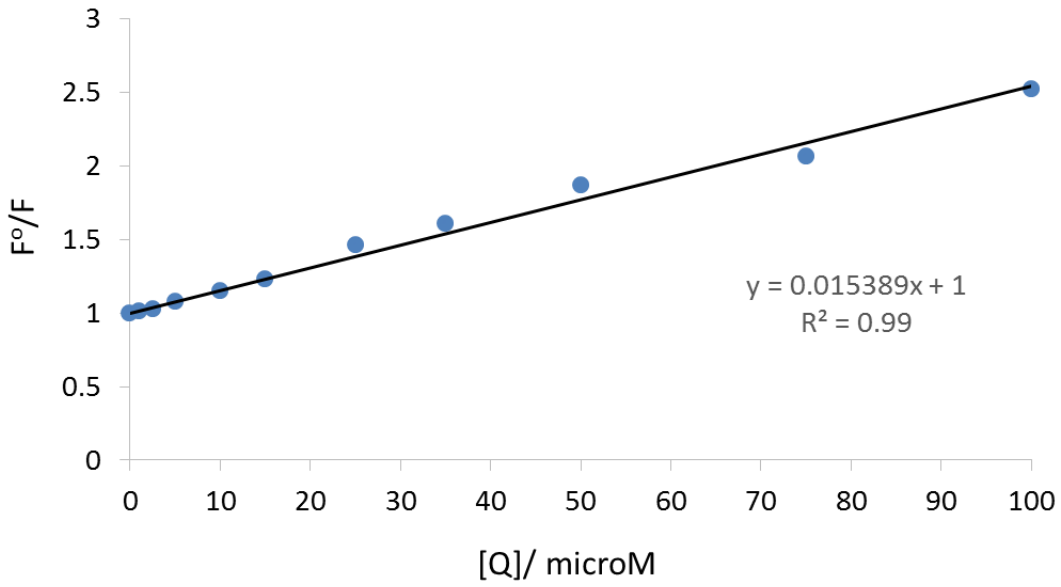

Figure S44. Representative F^o/F versus [Q] plot corresponding to the emission spectra for ethidium bromide (1 μM) bound to ct-DNA (1:20 ratio) upon addition of aliquots of **3**.

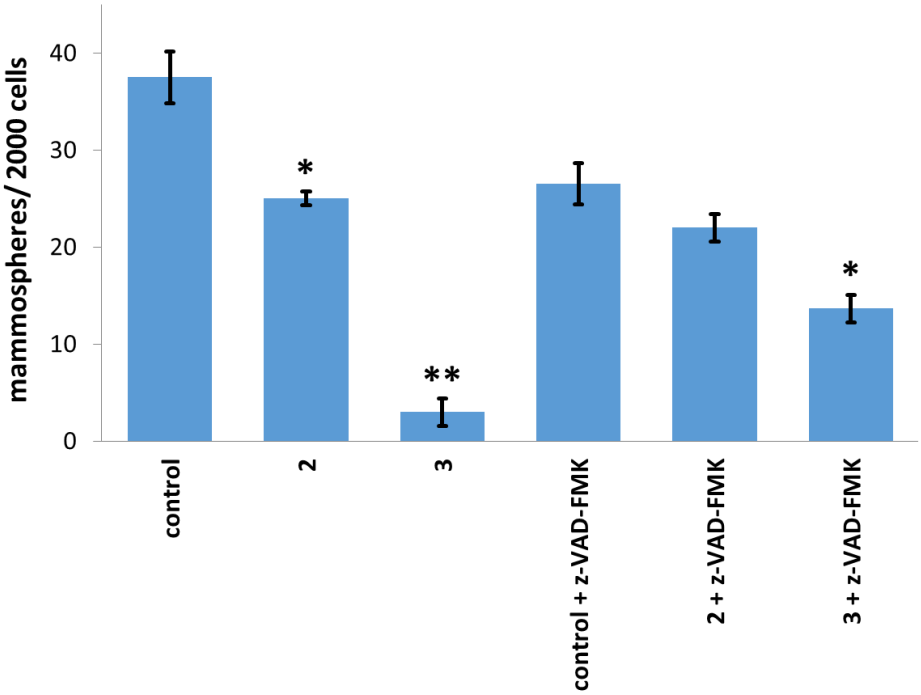

Figure S45. Quantification of mammosphere formation with HMLER-shEcad cells untreated and treated with **2** or **3** (at the IC_{20} value) only, and **2** or **3** (at the IC_{20} value) in the presence of z-VAD-FMK (5 μM) after 5 days incubation. Quantification of mammosphere formation with HMLER-shEcad cells treated with only z-VAD-FMK (5 μM) after 5 days incubation is also shown. Error bars = SD and Student t-test, * = $p < 0.05$, ** = $p < 0.01$.

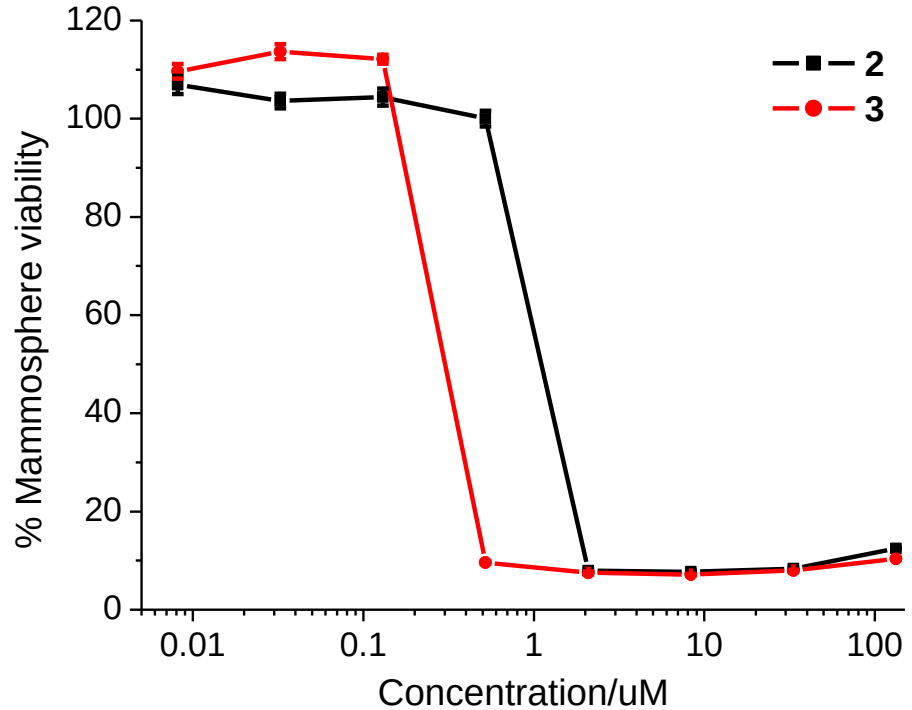

Figure S46. Representative dose-response curves for the treatment of HMLER-shEcad mammospheres with **2** or **3** in the presence of z-VAD-FMK (5 μM) after 5 days incubation.

References

[1] G. Sheldrick, *Acta Cryst.* **2008**, *A64*, 112-122.